National Defense
Defence nationale

DEFINITION OF THE CONCEPT OF AN INTERFEROMETRIC SPECTRUM ANALYSER FOR THE DETECTION OF FREQUENCY HOPPING RADIOS (U)

by

Nicole Brousseau

DEFENCE RESEARCH ESTABLISHMENT OTTAWA
TECHNICAL NOTE 90-20

Canada

October 1990
Ottawa

National Defence / Défense nationale

DEFINITION OF THE CONCEPT OF AN INTERFEROMETRIC SPECTRUM ANALYSER FOR THE DETECTION OF FREQUENCY HOPPING RADIOS (U)

by

Nicole Brousseau
Communications Electronic Warfare Section
Electronic Warfare Division

DEFENCE RESEARCH ESTABLISHMENT OTTAWA
TECHNICAL NOTE 90-20

PCN
041LK11

October 1990
Ottawa

ABSTRACT

The concept of a high resolution, large bandwidth and high dynamic range acousto–optic spectrum analyser for the detection of frequency hopping radios is described. The high resolution is achieved by selecting large time–aperture Bragg cells while the high dynamic range is obtained by using heterodyne detection in an interferometric structure. The large bandwidth is produced by a scanning process. An example of the probability of detection for a specific selection of parameters is given.

RESUME

Ce rapport contient une description du concept d'un analyseur de spectre acousto–optique à haute résolution, grande bande passante et à plage de linéarité étendue. La haute résolution provient de la sélection de cellules de Bragg ayant un grand temps d'interaction. La plage de linéarité étendue est le résultat de l'utilisation de détection hétérodyne dans une structure interférométrique pendant que la grande bande passante provient d'un procédé de balayage. On calcule un exemple de la probabilité de détection pour une sélection particulière de paramètres.

EXECUTIVE SUMMARY

The signal environment generated by the utilization of frequency hopping radios for military tactical communications is characterized by the presence of multiple emitters transmitting instantaneously narrow band signals, but changing their frequency of operation rapidly. The total bandwidth of operation of a frequency hopping radio network may be as large as 60 MHz and the size of the hops may be as small as 25 kHz. Thus, effective detection and analysis of frequency hopping signals requires a spectrum analyser capable of analysing 2400 frequency bins in parallel and in real time for the bandwidth of interest. Processing with a dynamic range of 60 dB is believed to be the minimum to obtain worthwhile results. The design and implementation of a spectrum analyser that could meet such demanding requirements is a formidable challenge and, although many analogue and digital approaches have been investigated, a definitive solution has yet to be found.

The purpose of this study is to define the concept of a high resolution, wide bandwidth and large dynamic range spectrum analyser based on an interferometric spectrum analyser (ISA) architecture to meet the spectral analysis requirements for the detection and analysis of frequency hoppers with slow to medium hop rates (10–1000 hops/sec). The total bandwidth of the proposed ISA is on the order of 50 MHz with a resolution of 25 kHz and the system operates with a dynamic range of at least 60 dB. The high resolution is achieved by selecting large time–aperture Bragg cells, while the high dynamic range is obtained by using heterodyne detection in an interferometric structure. The large bandwidth is produced by a scanning process. The probability of detection for a specific example is calculated and proposals for exploratory experimental work are presented.

TABLE OF CONTENTS

LIST OF FIGURES

LIST OF FIGURES (cont)

LIST OF ABBREVIATIONS

APD:	avalanche photodiode detector
CW:	continuous wave
He–Ne:	helium neon
IF:	intermediate frequency
ISA:	interferometric spectrum analyser
LO:	local oscillator
PNS:	pseudonoise sequence
PSA:	power spectrum analyser
RF:	radio frequency
SISA:	scanning interferometric spectrum analyser

1.0 INTRODUCTION

The addition of frequency hopping radios to conventional military tactical communications systems generates an environment that is characterized by the presence of multiple emitters transmitting instantaneously narrow band signals where some of the emitters change their frequency of operation rapidly. The total bandwidth of operation of a frequency hopping radio network may be as large as 60 MHz and the size of the hops may be as small as 25 kHz. Thus, effective detection and analysis of frequency hopping signals requires a spectrum analyser capable of analysing 2400 frequency bins in parallel and in real time for the bandwidth of interest. Processing with a dynamic range of 60 dB is believed to be the minimum to obtain worthwhile results. The design and implementation of a high probability of intercept spectrum analyser that could meet such demanding requirements is a formidable challenge and, although many analogue and digital approaches have been investigated, a definitive solution has yet to be found.

One of the promising approaches currently pursued by many research groups utilizes acousto–optic technology and heterodyne detection. The utilization of heterodyne detection doubles (in dB) the dynamic range of the detection process when compared to power detection. Such systems are called Interferometric Spectrum Analysers (ISA). A workable architecture was described for the first time by A. Vander Lugt in 1981 [1] where all elements of the detector array are producing a beat signal at the same IF. The concept of the ISA was further refined by Vander Lugt et al. [2,3] and experimental implementations were reported [4,5,6]. More theoretical and experimental studies on the origin of the limitations of the performances of the ISA have been published [7,8,9]. Recent experimental results [10] on the ISA demonstrate that the promise to double the dynamic range is realistic although not exactly fulfilled. Developing a capability for the detection of frequency hoppers is so important that exploratory work on ISAs is justified, although problems are already foreseen in the miniaturization and packaging of the system for field operation. Some serious difficulties are also anticipated in the design and implementation of the read–out circuitry for the detector array, in the beam–shaping optics for the illumination of the system, in the generation of a reference signal with appropriate characteristics and in the implementation of the scanning process utilized to extend the bandwidth of operation.

The purpose of this study is to define the concept of a high resolution, wide bandwidth and large dynamic range spectrum analyser based on the ISA architecture to meet the spectral analysis requirements for the detection and analysis of hoppers with slow to medium hop rates (10–1000 hops/sec). The total bandwidth of the ISA should be on the order of 60 MHz with a resolution of 25 kHz and the system should operate with a dynamic range of at least 60 dB. The principle of operation of a simple system, the Power Spectrum Analyser (PSA), will be briefly reviewed and utilized as a stepping stone for the analysis of a narrow band, high resolution ISA. Then the concept of a wideband ISA will be defined where the increased bandwidth is achieved by a scanning process. The probability of detection of the Scanning ISA (SISA) will be calculated as a function of the hop rate and, finally, plans will be outlined to undertake exploratory work on the characterization of the main components of the SISA to prepare the ground for development of a proof of concept system. That work will be based on facilities and recent technological advances available at DREO.

2.0 POWER SPECTRUM ANALYSER

The Power Spectrum Analyser (PSA) is the simplest implementation of a spectrum analyser using acousto–optic technology (see Fig. 1). A short description of the operation of a PSA with emphasis on the aspects that are relevant to the analysis of the ISA is useful as an introduction to the rest of the work.

In a PSA, as shown in Fig. 1, the down–converted RF signal is applied to the transducer and transformed into changes of index of refraction (acoustic waves) propagating through the Bragg cell. A parallel beam of coherent laser light illuminates the cell at the Bragg angle and some of the light is diffracted by the acoustic waves propagating across the Bragg cell. The angle of diffraction depends on the frequency of the RF signal applied to the transducer. A lens performs a Fourier transform of the diffracted light and the distribution of light formed in the Fourier plane is detected by an array of square law detectors whose response is linear with intensity. The resolution of the system is determined by the size of the detecting elements, the scale of the Fourier transform and the length and transit time of the signal in the Bragg cell. Ideally, the parameters of the system should be adjusted in such a way as to have two detecting elements within the width of the diffraction spot produced by a Continuous Waveform (CW) signal filling the aperture of the Bragg cell. If that condition is met, one can truly say [1] that the resolution R of the system is

$$R = 1/\tau \qquad (1)$$

where τ is the transit time of the signal in the Bragg cell. This statement applies to both the PSA and the ISA. The dynamic range of a PSA is usually between 30–40 dB and is limited by either the dynamic range of the detector array or the intermodulation products generated in the Bragg cell. Also, in a PSA, the photodetector current is proportional to the square of the RF signal amplitude.

Finally there is one more aspect of the acousto–optic interaction that is of crucial importance to the design of an ISA: the light diffracted by the Bragg cell is frequency shifted (Doppler effect) by an amount equal to the frequency of the acoustic wave it interacted with. This is the basis of the design of an ISA and a good understanding of the temporal frequency shift of the diffraction patterns produced by CW signals and pulses is very important for the study of the characteristics of the beat signal produced in an ISA. Four cases of interest are analysed in Appendix A: the case of CW signals filling the Bragg cell, the case of pulses all within the Bragg cell and the case of CW signals either entering or leaving the Bragg cell.

The results can be summarized as follows: in all cases the temporal frequency f_o of the laser light diffracted at the center of the diffraction pattern is shifted by the frequency f_a of the acoustic signal in the Bragg cell. When the Bragg cell is filled with a CW signal, all the sidelobes of the diffraction pattern oscillate at the same temporal frequency f_o+f_a as the center of the diffraction pattern. When both the leading and trailing edges of a pulse of frequency f_a are within the Bragg cell, the temporal frequency of the sidelobes is no longer at the same frequency as the center of the diffraction pattern: at some spatial frequency $f_a+\Delta f$, the temporal frequency is $f_o+f_a+\Delta f$. Finally, when only the leading or the trailing edge of a pulse of frequency f_a is within the Bragg cell, the temporal frequency of the sidelobes at a spatial frequency $f_a+\Delta f$ is $f_o+f_a+\Delta f/2$.

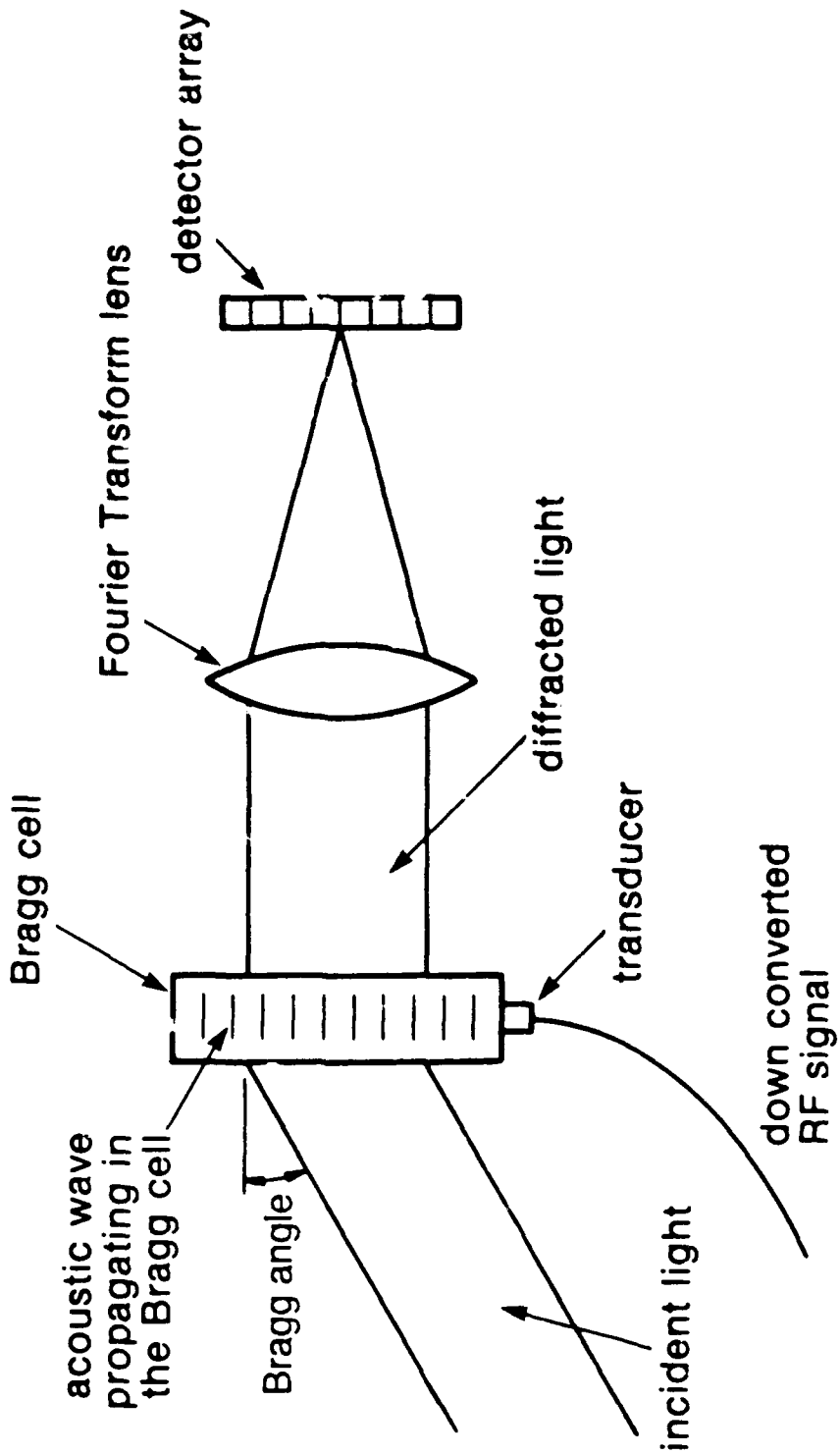

FIGURE 1: THE POWER SPECTRUM ANALYSER

time: t_0

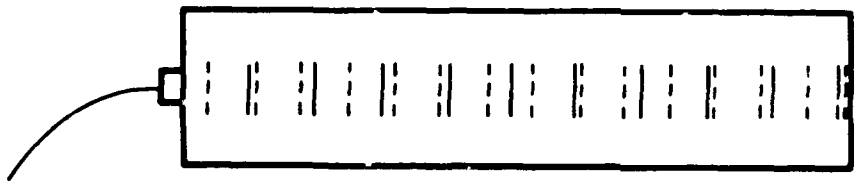

two waves filling the Bragg cell at $t = t_0$

a)

time: $t_0 + \delta$

two waves filling the Bragg cell at $t = t_0 + \delta$

b)

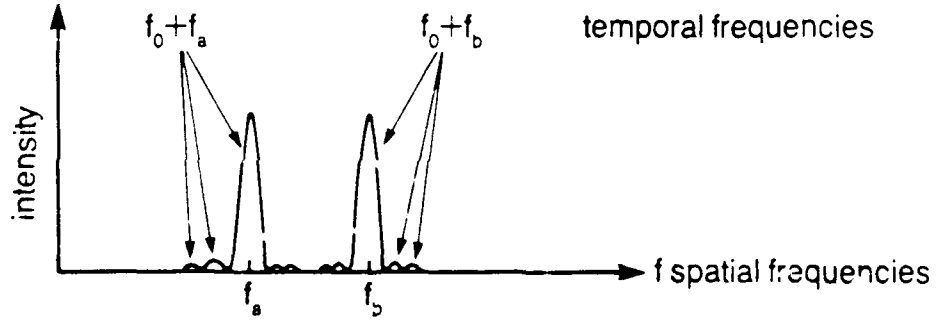

instantaneous spectrum at $t = t_0$ and $t = t_0 + \delta$

c)

FIGURE 2: DOPPLER FREQUENCY SHIFT OF THE DIFFRACTION PATTERNS OF CW SIGNALS WHEN THE CW SIGNALS FILL THE BRAGG CELL

Fig. 2a illustrates two CW signals at different frequencies f_a and f_b and their respective spectra at time t_o. The two spectra, including the main lobes and the sidelobes, are oscillating respectively at the temporal frequencies f_o+f_a and f_a+f_b. Fig. 2b illustrates the situation at a later time $t_o + \delta$. The two CW signals have propagated through the Bragg cell, but they still fill the cell and the spectra (see Fig. 2 c) are the same as at time t $= t_o$.

In Fig. 3a, two short pulses at different frequencies f_a and f_b are within the aperture of the Bragg cell at time $t = t_o$. The two pulses have difference lengths L_a and L_b so their Fourier transforms have different widths and amplitudes. The spectral centers (see Fig. 3c) of the pulses are oscillating, as in the previous case, at the temporal frequencies of f_o+f_a and f_o+f_b, but at a distance Δf from the center of the main lobes, the temporal frequencies of the two diffraction patterns are $f_o + f_a + \Delta f$ and $f_o + f_b + \Delta f$. In Fig. 3b, the two pulses, at time $_o + \delta$, are still within the aperture of the Bragg cell so their lengths are the same and the widths of their diffraction patterns and the temporal frequency characteristics are identical to the case illustrated in Fig. 3a.

Fig. 4a illustrates, at time $t = t_o$, two CW signals of frequencies f_a and f_b entering the Bragg cell. At time $t = t_o$, the length of the CW signals entering the cell are L_a and L_b. The spectra (see Fig. 4c) thus have different widths and amplitudes but the centers of the main lobes are oscillating at the temporal frequencies $f_o + f_a$ and $f_o + f_b$ respectively. At a distance Δf from the center of the main lobes of the two diffraction patterns, the temporal frequencies are $f_o + f_b + \Delta f/2$. In Fig. 4b, the two CW signals are illustrated a few moments later at $t = t_o + \delta$. The lengths of the CW signals within the cell are greater and now equal to $L_a + \delta v$ and $L_b + \delta v$, where v is the velocity of the acoustic wave in the Bragg cell. The width of the diffraction patterns of the CW signals is thus narrower and the intensity larger, but the distribution of the temporal frequencies on the diffraction pattern is the same as in Fig. 4a.

Fig. 5a illustrates, at time $t = t_o$, two CW signals of frequenc f_a and f_b, leaving the Bragg cell. At time $t = t_o$, the lengths of the CW signals within the cell are L_a and L_b. The spectra (see Fig. 5c) have different amplitudes and widths but the centers of the mainlobes are oscillating at a temporal frequency of $f_o + f_a$ and $f_o + f_b$. At a distance Δf from the main lobes of the two patterns, the temporal frequencies are $f_o + f_a + \Delta f/2$ and $f_o + f_b + \Delta f/2$. In Fig. 5b, the two CW signals are illustrated a few moments later at time $t = t_o + \delta$. The lengths of the CW signals within the cells are now $L_a - \delta v$ and $L_b - \delta v$. The widths of the diffraction patterns are now larger and their intensity is smaller, but the distribution of the temporal frequencies on the diffraction pattern is the same as for the cases illustrated in Figs. 4a, 4b and 5a.

3.0 PRINCIPLES OF OPERATION OF AN INTERFEROMETRIC SPECTRUM ANALYSER

The general principles of operation of an ISA and the relationship between some of the parameters of the design will be discussed in this section. A workable architecture for an ISA was first proposed by Vander Lugt [1] in 1981. It is based on the heterodyne mixing of the spectrum of a reference with the spectrum of the signal to be analysed. The breakthrough in the implementation proposed by Vander Lugt is an ingenious architecture where each element of the detector array produces a beat signal at the same IF. The ISA is expected to provide an improvement of the dynamic range by a factor of 2 (in dB) when compared to the PSA.

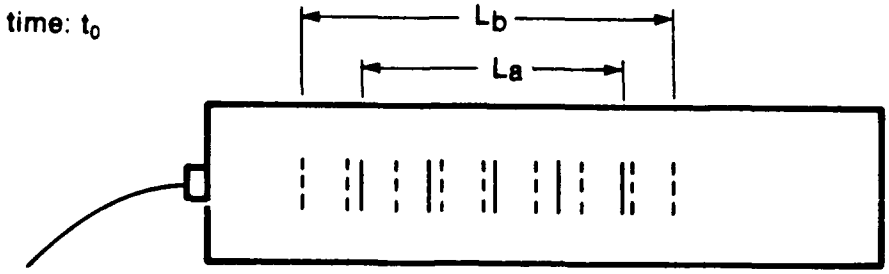

two short pulses within the Bragg cell at $t = t_0$

a)

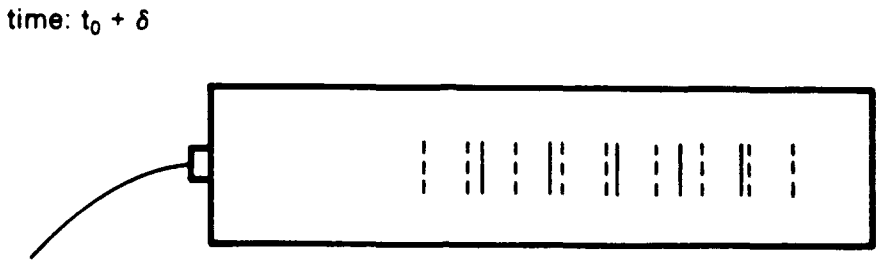

two short pulses within the Bragg cell at $t = t_0 + \delta$

b)

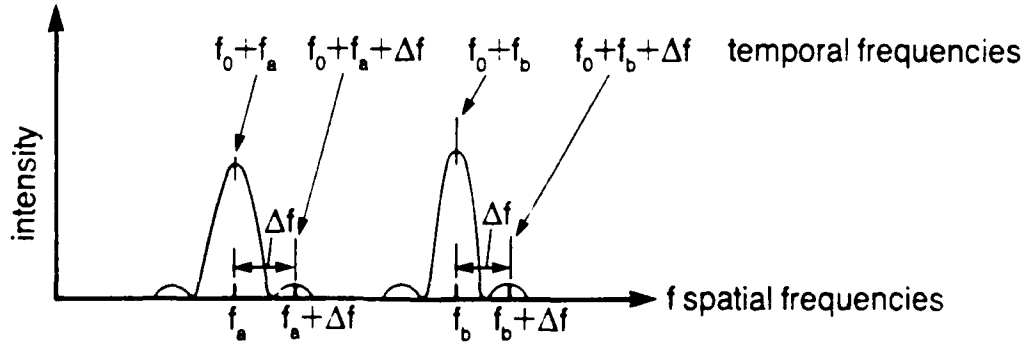

instantaneous spectrum at $t = t_0$ and $t = t_0 + \delta$

c)

FIGURE 3: DOPPLER FREQUENCY SHIFT OF THE DIFFRACTION PATTERNS OF CW SIGNALS WHEN SHORT SIGNALS ARE ALL WITHIN THE BRAGG CELL

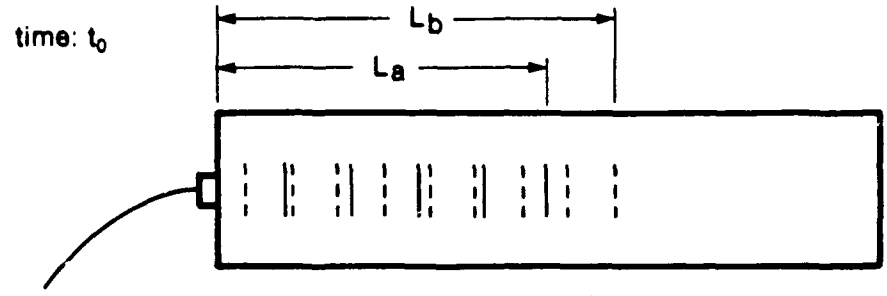

two waves entering the Bragg cell at $t = t_0$

a)

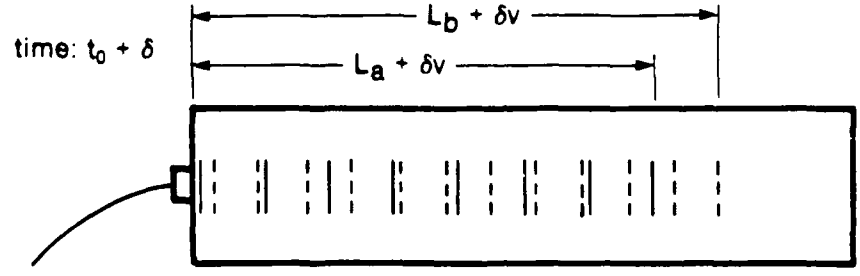

two waves entering the Bragg cell at $t = t_0 + \delta$

b)

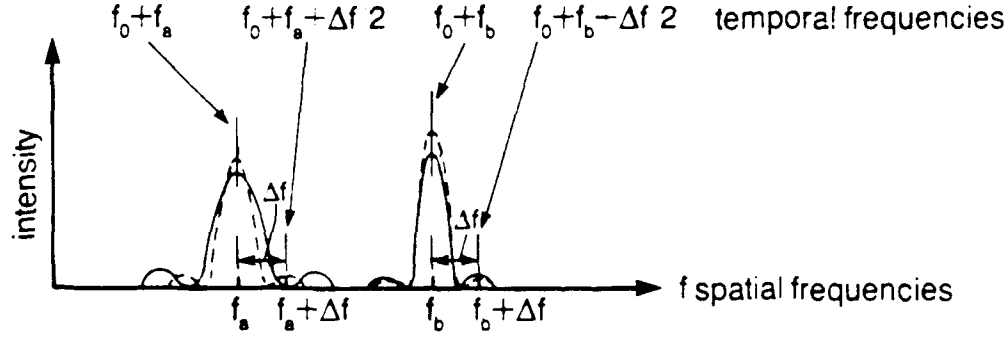

instantaneous spectrum at $t = t_0$ (-) and $t = t_0 + \delta$ (---)

c)

FIGURE 4: DOPPLER FREQUENCY SHIFT OF THE DIFFRACTION PATTERNS OF CW SIGNALS WHEN THE CW SIGNALS ARE ENTERING THE BRAGG CELL

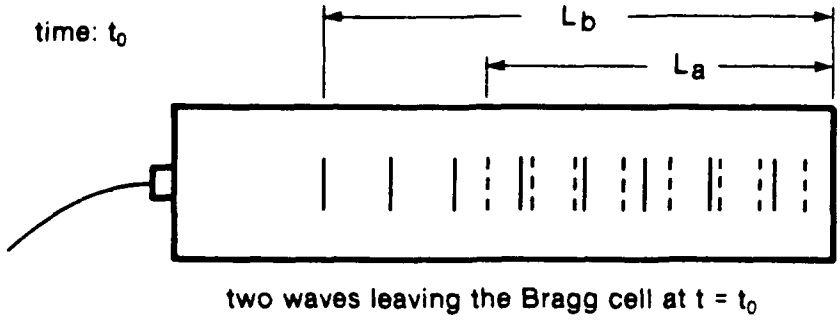

two waves leaving the Bragg cell at $t = t_0$

a)

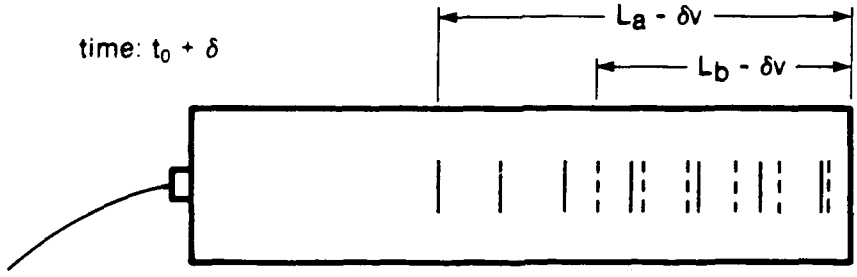

two waves leaving the Bragg cell at $t = t_0 + \delta$

b)

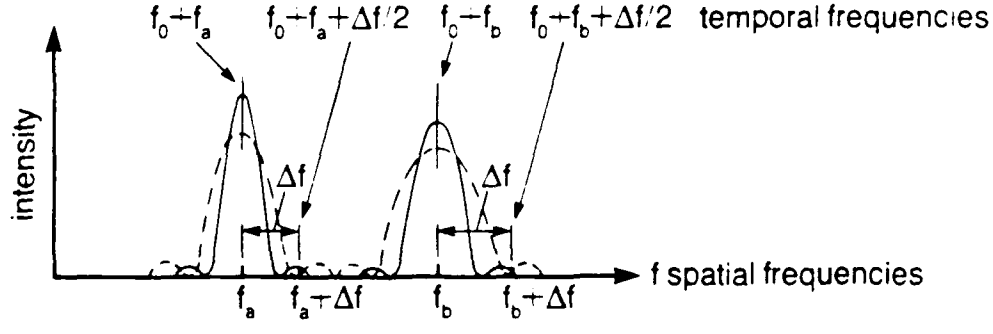

instantaneous spectrum at $t = t_0$ (-) and $t = t_0 + \delta$ (---)

c)

FIGURE 5: DOPPLER FREQUENCY SHIFT OF THE DIFFRACTION PATTERNS OF CW SIGNALS WHEN THE SIGNALS ARE LEAVING THE BRAGG CELL

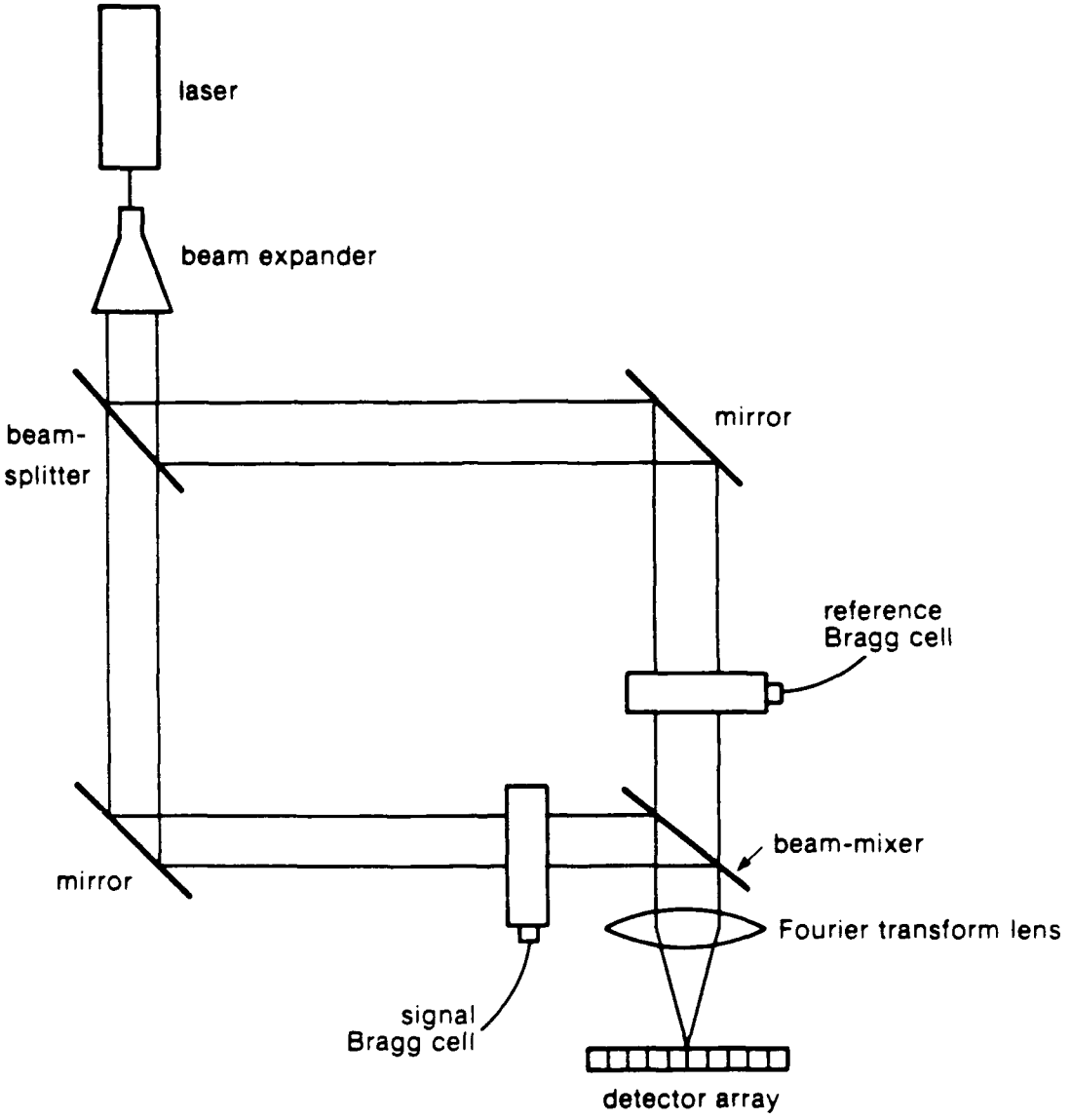

FIGURE 6: THE INTERFEROMETRIC SPECTRUM ANALYSER: MODIFIED MACH–ZENDER ARCHITECTURE

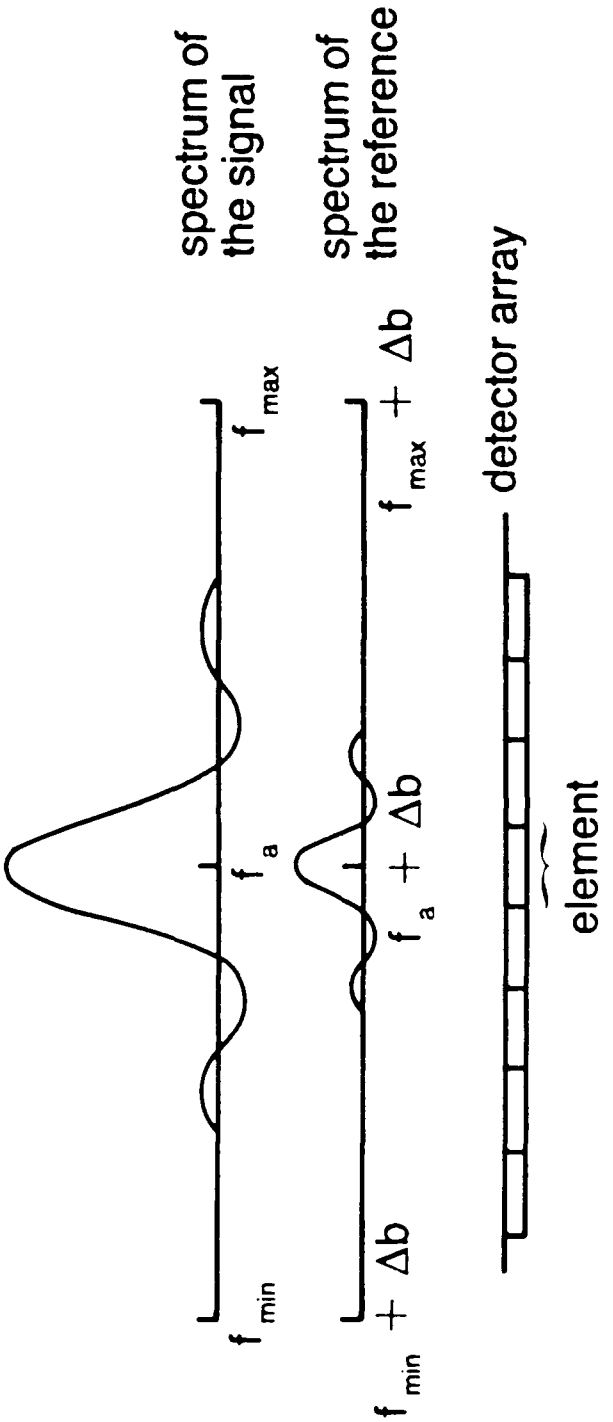

FIGURE 7: FOURIER PLANE OF AN ISA

An ISA can be implemented by adding to the simple PSA structure a reference arm designed to produce an appropriate reference to heterodyne with the spectrum of the signal (see Fig. 6). In such a system, the light from a laser is expanded and separated into two paths by a beam splitter. Each path is folded by mirrors and interacts with a Bragg cell. The signal to be analysed is applied to one of the Bragg cells while a reference is applied to the other Bragg cell. The laser beams diffracted by the two Bragg cells are mixed in such a way as to introduce, by a careful rotation of the beam mixer, a spatial displacement between the spectra of the two signals. Because the temporal frequency of the light diffracted by a CW signal at a frequency f_a is frequency shifted by the same amount f_a, each position in the Fourier plan corresponds to a different temporal frequency. A similar distribution of frequencies occurs in the Fourier plan of the reference. The spatial displacement introduced by the rotation of the beam mixer ensures that the light from the signal at a spatial frequency f_a and temporal frequency f_o+f_a is coincident with light from the reference at a spatial frequency $f_a+\Delta b$ and temporal frequency $f_o+f_a+\Delta b$ where Δb is the frequency displacement between the spectra (see Fig. 7) introduced by the rotation of the beam mixer. If s(p,t) and r(p,t) represent the signal and the reference in the Fourier plane, a square law photodetector will produce a signal u(p,t)

$$\begin{aligned} u(p,t) &= |s(p,t) + r(p,t)|^2 \\ &= |s(p,t)^2 + |r(p,t)|^2 + 2\,Re(s(p,t)r^*(p,t)) \end{aligned} \tag{2}$$

where * denotes complex conjugate and Re, the real parts. The overlapping parts of s(p,t) and r(p,t) are oscillating at the temporal frequency $f_s=f_o+f_a$ and $f_r=f_o+f_a+\Delta b$ respectively, so the third term of Eq. (2), $2Re(s(p,t)r^*(p,t))$ has a carrier frequency at

$$f_s+f_r = 2f_o + 2f_a + \Delta b \tag{3}$$

or at

$$f_s-f_r = \Delta b \tag{4}$$

In the second case, the difference $f_s-f_r = \Delta b$ depends only on the geometrical alignment of the beam mixer which can be adjusted to a conveniently low frequency.

One can also notice from Eq. (2) that, given a constant reference level, the photodetector current generated by the third term, the heterodyne term, is proportional to the RF signal rather than its square, as in the case for a PSA. However, the dynamic range of a light detector is always specified in terms of the intensity of the incident light. Thus, for a given detector, the dynamic range of a heterodyne detection process is, theoretically, twice (in dB) the dynamic range of square law detection. For example, if a detector has a dynamic range of 100 (20 dB) when used to detect a light distribution intensity that is proportional to the square of the RF applied to the Bragg cell, the same detector will be able to measure a dynamic range of 10000 (40 dB) as a heterodyne detector because, in that case, the reference is kept constant and the current produced by the detector is proportional the RF signal. Naturally, the detecting elements and their read–out circuitry will have to be fast enough to respond to the chosen beat frequency. Avalanche Photodiode Detectors (APDs) are now available in linear arrays and offer an advantage of approximately 13 dB in equivalent noise power over PIN detectors [6,11]. It is also advisable to add a bandpass filter at the output of each element of the detector array to increase the frequency discrimination of the ISA and to reduce the noise level by

filtering out signals that are not oscillating at the beat frequency. These include scattered undiffracted light and diffracted light that has been scattered sufficiently far from its intended beam. The ISA will thus exhibit an improved immunity to noise when compared to the PSA.

Selection of a reference signal is a very important design criteria for an ISA. A reference should have a spectrum of uniform intensity over the operational bandwidth of the ISA in order to produce uniform sensitivity. Then its spectrum, if not constant in time, should at least not have temporal frequencies within the bandwidth of the filter centered at the beat frequency Δb selected for operation to ensure uniformity of operation over time. Also, light should be used efficiently and, if reference signals are only used periodically, the duty cycle should be high so that short duration pulses are not missed.

At first glance, quite a few types of references have spectra that seem to be suitable candidates for an ISA: a narrow pulse, white or Gaussian noise, combs of discrete, equally spaced frequencies and repetitive waveforms such as pseudorandom noise sequences (PNSs) or chirps. It is possible to eliminate the first two candidates for simple reasons: narrow pulses have suitable spectra but do not use light effectively because they occupy only a small part of the Bragg cell. White or Gaussian noise has a spectrum that fluctuates too much to provide the spatial and temporal uniformity required of the detection process. Combs of discrete frequencies are conceptually very attractive but they are difficult to implement because the amplitude of the intermodulation products must be kept below the level of the combs by at least the expected dynamic range of the system. If repetitive waveforms are used, their repetition rates should be such that no harmonics occur near the ISA's IF or else spurious signals may occur within the detection bandwidth. Also, the aperture of the Bragg cell should contain an integer number of waveforms in order to produce a spatially uniform spectral distribution in the Fourier plane. PNSs have been used successfully [6] in the demonstration of ISAs although the magnitudes of the spectra at a particular frequency may fluctuate in time by a substantial amount (see Fig. 8) as the PNSs propagate through the Bragg cell. Spatial fluctuations also occur across the Fourier plane and depend on the parameters of the sequence (see Fig. 9). Chirps are very interesting references for an ISA. Simulations implemented by Wilby et al. [7] have shown that apart from the Fresnel ripple at the band edges, they produced, in an ideal situation, the best spectral uniformity. They have also been used successfully in experimental work [5,10].

The resolution of the ISA is determined by the size of the diffraction patterns produced by the Bragg cells and by the size of the elements of the detector array. In order to have a frequency resolution of R, the width of the diffraction pattern produced by the signal Bragg cell has to be at least twice the width of one detecting element (see Fig. 7). A consequence of this statement is that a system with a large bandwidth and fine resolution requires a large number of detecting elements. If a comb of frequencies is used as a reference, one frequency is required for each element of the detector array. If too much overlap between adjacent reference diffraction patterns is to be avoided, the reference Bragg cell has to be about twice as long as the signal Bragg cell in order to produce diffraction patterns that are about half the size of the signal diffraction patterns.

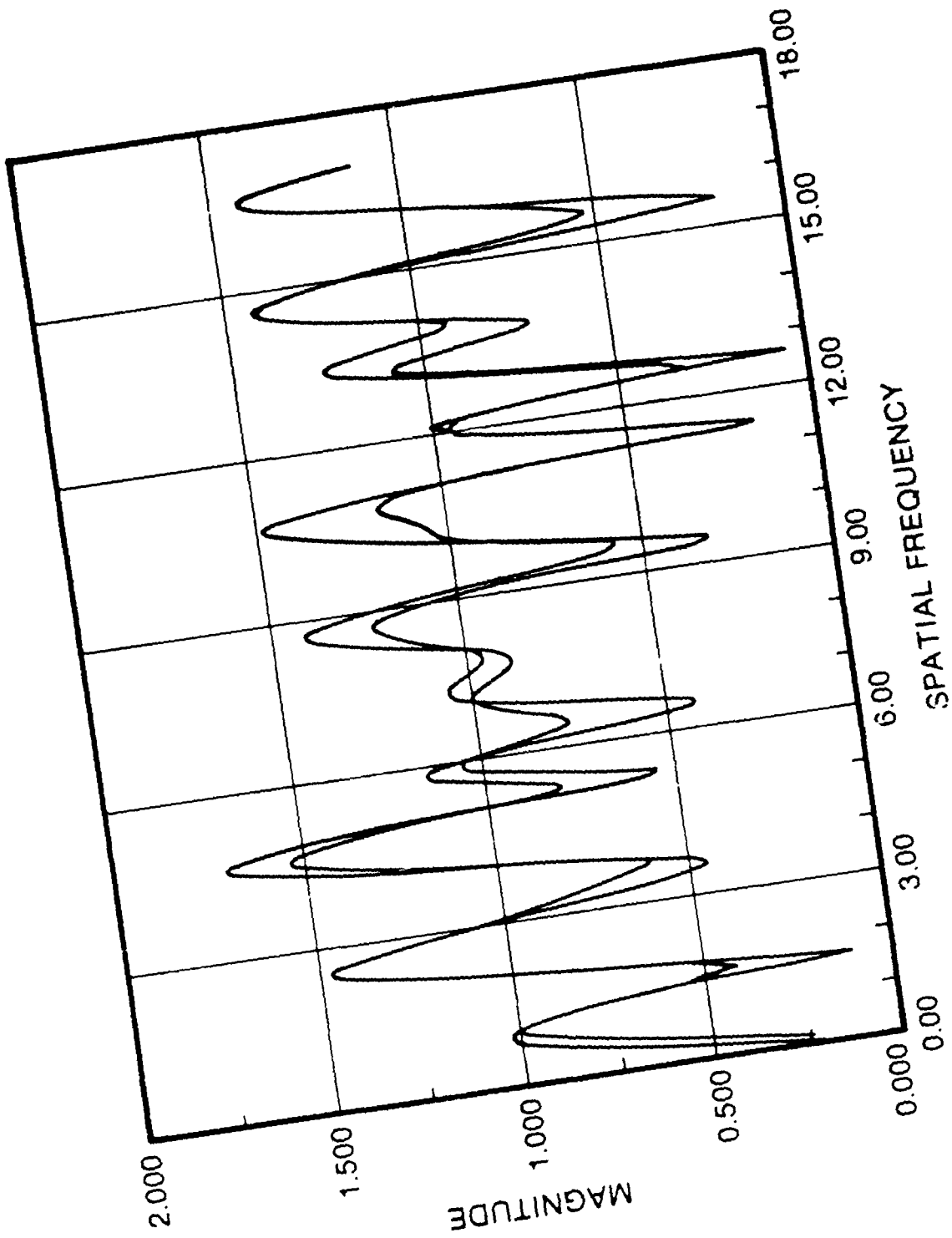

FIGURE 8: MAGNITUDE OF THE FOURIER TRANSFORM OF A PSEUDONOISE SEQUENCE FOR TWO ADJACENT SHIFT POSITIONS (FROM [1], p. 2776)

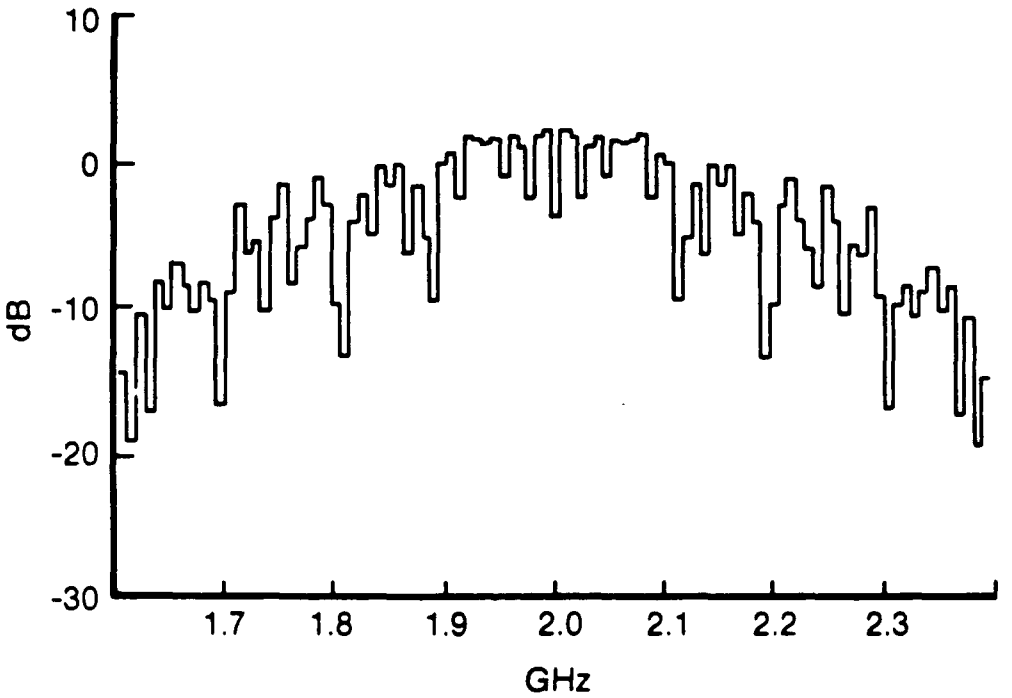

FIGURE 9A: REFERENCE SPECTRUM FOR A PSEUDONOISE CODE USING A 7–REGISTER M–SEQUENCE AND 2 ns CHIP LENGTH IN A 160 ns UNIFORM APERTURE (FROM [7], p. 52)

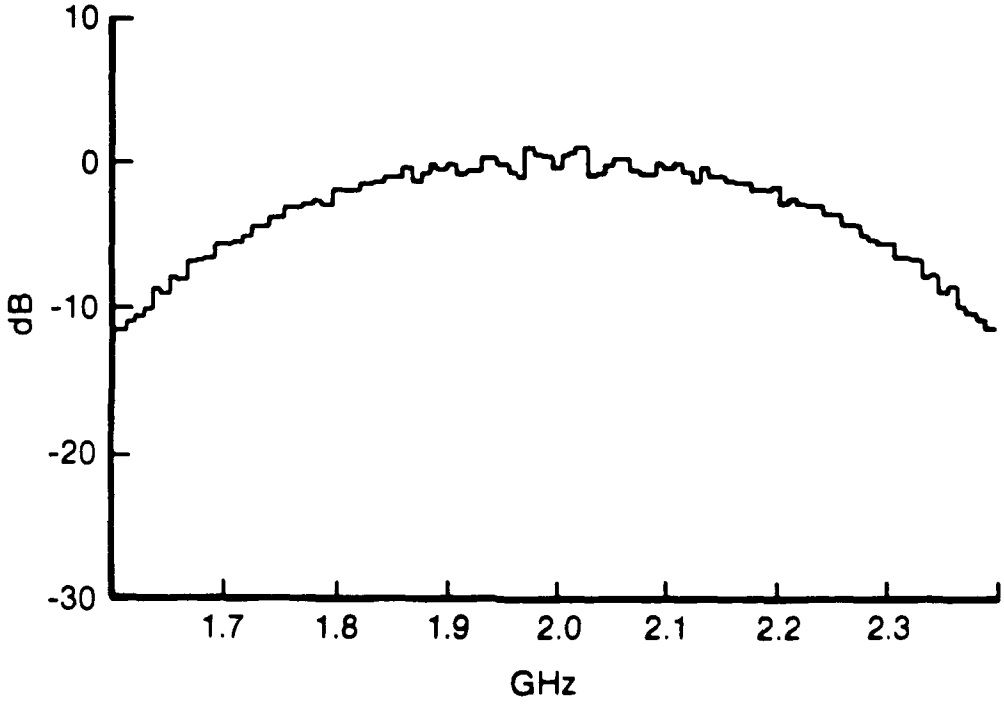

FIGURE 9B: REFERENCE SPECTRUM FOR A PSEUDONOISE CODE USING A 9–REGISTER M–SEQUENCE AND 2 ns CHIP LENGTH IN A 1 μs UNIFORM APERTURE (FROM [7], p. 52)

In the above section, many factors pertaining to the general operation of an ISA were reviewed. The increase in dynamic range associated with the utilization of a reference and with the heterodyne detection process was discussed together with the factors having an impact on the selection of a reference signal. The main factor influencing the resolution of the ISA and the advantages of filtering the beat signals detected by the elements of the detector array were also mentioned. In the next section, a specific design for a high resolution ISA operating with a narrow bandwidth will be developed from the general principles outlined in Section 3.

4.0 CONCEPT FOR A HIGH RESOLUTION INTERFEROMETRIC SPECTRUM ANALYSER

Detection of all the hops from a typical frequency hopping radio such as the Racal Jaguar V requires a resolution of 25 kHz over a bandwidth of 60 MHz. Obtaining such a resolution over a 60 MHz bandwidth with a dynamic range of 60 dB from a spectrum analyser based on acousto–optic interactions is not an easy task. The purpose of this section is to develop a specific design for the optical system of an acousto–optic ISA that could meet the resolution and dynamic range requirements for detection of frequency hoppers. The bandwidth of the system described in this section will be inadequate to cover 60 MHz but a modification to the operation will be introduced in Section 5 to provide a large bandwidth capability.

The resolution of a Bragg cell, under the best conditions, is equal to $1/\tau$, where τ is the transit time of the acoustic signal across the Bragg cell. A spot size with a width of 25 kHz in the Fourier plane therefore requires a transit time of 40 μs. However, in order to genuinely resolve 25 kHz, two measurements have to be taken by the detector array within the 25 kHz spot size. If a comb of equally spaced frequencies is used as a reference signal, the spot size for each frequency of the comb has to be 12.5 kHz wide and the transit time of the signal into the reference Bragg cell is then 80 μs. If no scanning process is utilized, or if a chirp or pseudonoise sequence is utilized, the scale of the Fourier transform should be such that each element of the detector array sees a bandwidth of 12.5 kHz. A total of 4800 elements are then required to cover a 60 MHz bandwidth. This number of elements is an unrealistic requirement and large bandwidths have to be achieved by other means.

The only commercially available Bragg cells that have transit times on the order of 80–100 μ are made of TeO_2 [12]. They operate in the slow shear mode and the acoustic signal propagates at a velocity of 620 m/s. Bragg cell apertures of 24.8, 49.6 and 62 mm are available corresponding to 40, 80 and 100 μs transit times respectively. TeO_2 Bragg cells are available with surfaces polished to good optical quality ($\lambda/6$) and typical bandwidths of 30 or 50 MHz centered at 45 or 75 MHz respectively. The properties of large aperture TeO_2 Bragg cells, such as acoustic attenuation, intermodulation products and polarization effects, have been extensively studied [12,13,14]. The dynamic range of the signal diffracted by a TeO_2 Bragg cell operated at 75 MHz with a diffraction efficiency of 1% is illustrated in Fig. 10 as a function of the time aperture. The curve always stays above 35 dB even for very large time apertures. One can then conclude that a TeO_2 Bragg cell should be able to provide at least 70 dB of dynamic range when utilized in an ISA configuration with heterodyne detection.

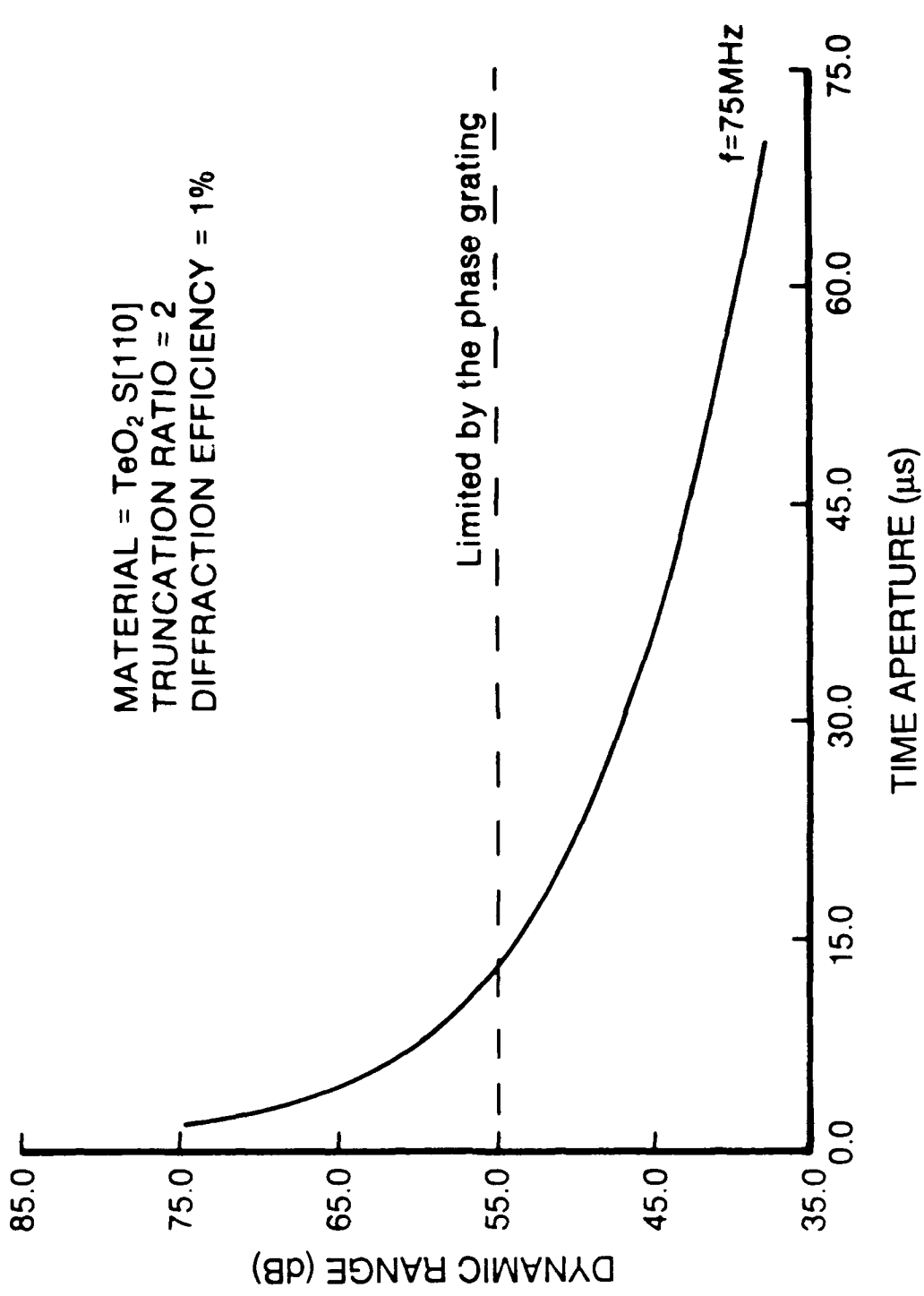

FIGURE 10: DYNAMIC RANGE IN INTENSITY OF A T_eO_2 BRAGG CELL IN THE SHEAR MODE FOR DIFFERENT TIME APERTURES (FROM [12], p. 146)

TeO_2 Bragg cells also exhibit interesting polarization properties [14]. An incident beam with right ellipticity of approximately 0.86 yields the maximum diffraction efficiency and is converted into left circularly polarized diffracted light. The polarization of the undiffracted light is not modified. It is thus possible to filter out scatter of undiffracted light with retardation plates and polarizers. A 13 dB reduction in background scattering has been reported [14]. However, it is difficult to find retardation plates and polarizers larger than 30 mm in diameter with good optical flatness and low scattering. Also, the gain in S/N ratio that should arise from polarization control in an ISA may be difficult to fully achieve. TeO_2 Bragg cells for use with linearly polarized input beams are under development [15] and should provide a distinct advantage when available.

Let us now make a few assumptions that will define the particular frequency hopper problem that is addressed here. We will assume that the hop rate of the received signals is relatively slow such that each hop generates a CW signal that fills the Bragg cell. Under these conditions, the main lobe and all the sidelobes of the diffraction pattern produced by a particular hop will oscillate at the same temporal frequency. For the narrow bandwidth ISA considered here, two types of reference signals seem particularly appropriate. First, a chirp of proper bandwidth and center frequency applied to the reference Bragg cell will produce a continuum of frequencies in the Fourier plane. The beat produced by heterodyning the diffraction pattern from a hop and the continuum of frequencies from the reference will generate a signal whose bandwidth is the same as the bandwidth seen by each element of the detector array (see Fig. 11a). The bandwidth of the bandpass filter following each element of the detector array should just allow the signal to pass. A second interesting reference signal is a comb of equally spaced frequencies (see Fig. 11b). In this case, each of the CW signals making up the comb produces a diffraction pattern where the main lobe and all the sidelobes oscillate at the same temporal frequency. The diffraction pattern produced by the CW signal from the hop is broader but has the same characteristics. The beat signal produced by one element of the detector array will be very narrow, but its center frequency may vary depending on the position of the centre of the signal being analysed. In this case also, the bandwidth of the filter should be similar to the bandwidth seen by each element of the detector array. With both the chirp and the comb reference, the efficiency of the heterodyne process will depend on the sensitivity profile of the detector array element and on the precise location of the hopper's signal relative to the detecting elements. If there are dead spaces between the elements, the ISA could be partially or totally blind to certain frequencies.

Among the prime considerations in the successful development of an ISA is the packaging of a system for field operation. The packaging of an interferometric structure requires careful construction especially when large apertures are involved. If a Mach–Zender configuration is used, a lot of parts are involved (see Fig. 12a). More glass surfaces means more scattering, more noise and poorer performance. A simpler configuration using a minimum of components was proposed [16] where the two folding mirrors and the two beam splitters of the Mach–Zender configuration are replaced by only two beam splitter cubes (see Fig. 12b). The resulting system will generate less scatter noise and be more compact and easier to package. It is possible with both architectures to produce two Fourier planes where a detector array can be placed. Thus, the achievable system bandwidth, using a given array with a limited number elements, can be doubled without sacrificing resolution.

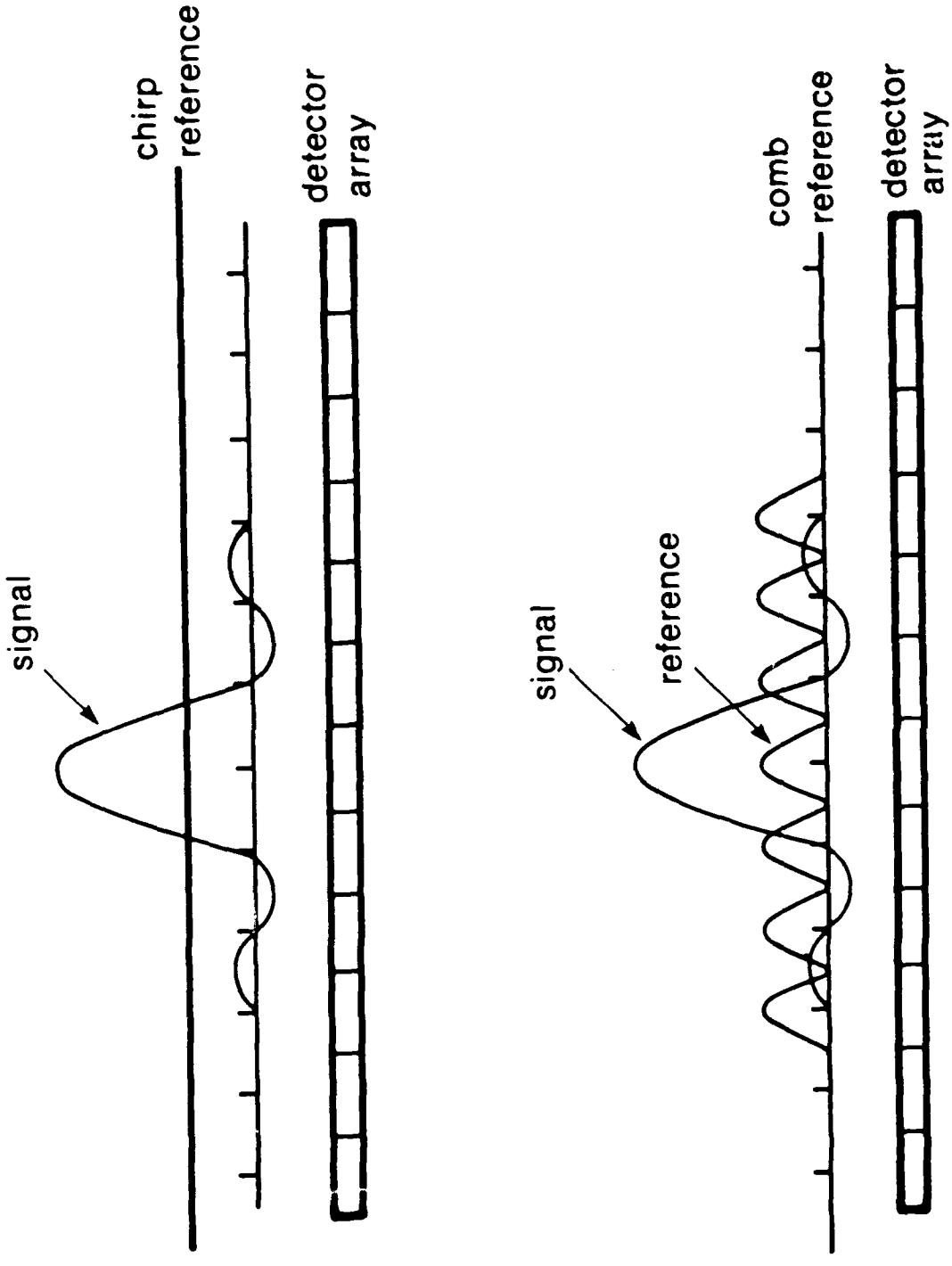

FIGURE 11: HETERODYNE PROCESS FOR
a) A CHIRP REFERENCE AND
b) A COMB OF EQUALLY SPACED FREQUENCIES

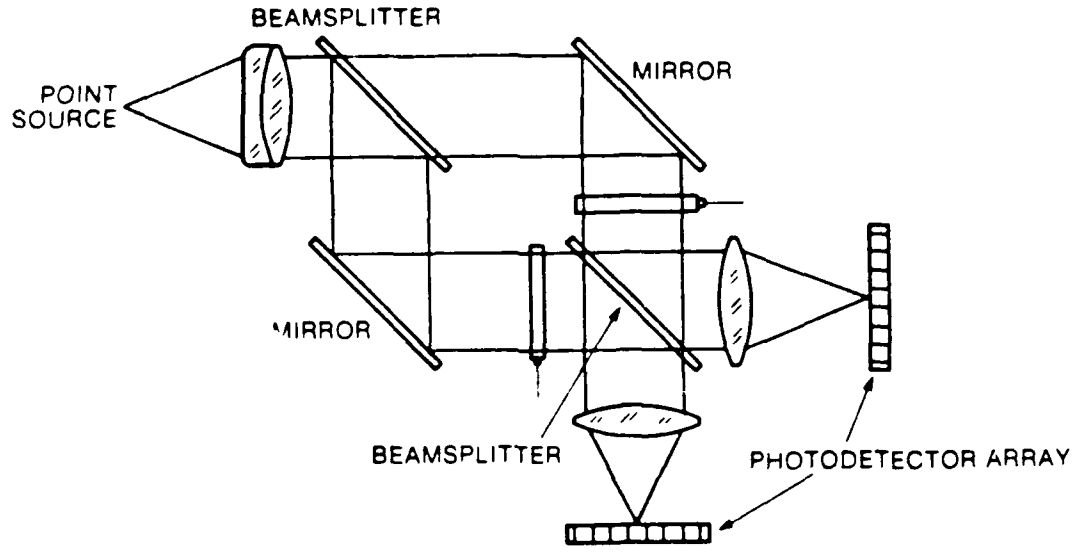

a)

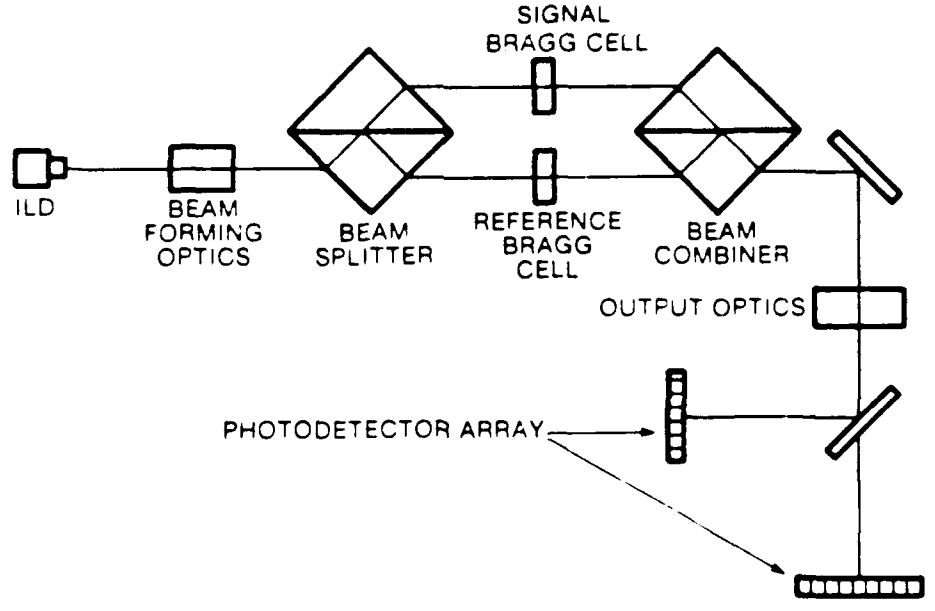

b)

FIGURE 12: ARCHITECTURE FOR AN ISA:
a) MODIFIED MACH–ZENDER
b) MINIATURE ISA

The beam shaping system used to expand the size of the laser beam has also to be considered carefully. Although a solid state laser is essential to the operation of a fielded system, we will use a He–Ne laser in the early stages of development because it is readily available in the laboratory for the preliminary tests. It can be easily verified (see Appendix B) that the multi–longitudinal mode structure of the He–Ne laser will not be detrimental to the operation of the ISA. The simple solution of using only a 100 mm diameter commercial spherical beam expander for a large apertures ISA is not acceptable: too much light is lost because of the anamorphic mismatch between the rectangular aperture of the Bragg cell (2 mm x 60 mm) and the circular shape of the illuminating beam. Anamorphic beam expansion is necessary. Prisms have the ability of compressing or expanding one dimension of a beam depending on the refraction geometry [17]. When used in their optimal geometry, prisms can provide expansion and compression ratios up to the value of their index of refraction. They also have the advantage of being easy to manufacture in large sizes because they are made only of flat surfaces. An interesting approach would be to first expand a He–Ne laser beam with a 50 mm diameter commercial spherical beam expander. After that first step, which includes the pinhole filtering of the laser output, the 50 mm circular beam could be expressed once or twice in one direction and expanded in the other direction with appropriate prisms. The shape of the illumination would then match the 2 mm x 60 mm aperture of the Bragg cell much better and produce a better light budget than if a 100 mm diameter beam expander was used.

In the high resolution, low bandwidth system considered in this section, one spot size of the reference signal (12.5 kHz wide) covers one element of the detector array. If the array of APDs produced by RCA with 150 μm wide elements is utilized, the focal length of the lens making the Fourier transform will be impractically long (5 m). The bandwidth of the ISA is also limited to 800 kHz if two 32–elements arrays are used. Such a small bandwidth is not useful for the frequency hopper problem addressed here. However, it is possible to increase the bandwidth of the system by designing a scanning process that will, on one hand, somewhat reduce the probability of detection of fast hoppers, but produce a bandwidth appropriate for a high probability of detection of slower hoppers. The next section contains a discussion of the concept of a Scanning ISA (SISA).

5.0 CONCEPT FOR A BROADBAND HIGH RESOLUTION INTERFEROMETRIC SPECTRUM ANALYSER

The purpose of this section is to define the concept of a large bandwidth, high resolution ISA. Scanning strategies have been proposed [3,18] to increase the bandwidth of an ISA, but, for several reasons, they are not appropriate for the specific problem considered here. A different approach for a Scanning Interferometric Spectrum Analyser (SISA) was therefore developed to fulfill our requirements. The increased bandwidth is achieved by a scanning process while the high resolution of the ISA described in Section 4 is retained. However, there is a price to pay for the larger bandwidth in terms of reduced probability of detection for fast hoppers. An array of APDs manufactured by RCA and the TeO_2 Bragg cells with a 45 MHz bandwidth centered at 75 MHz are retained as the main optical components of the system.

The architecture of the SISA is very similar to the set–up described for the ISA in Section 4. The main difference is that the focal length F of the Fourier transform lens is much shorter, so the width of the reference signal occupies only a small fraction of the width of one detecting element (see Fig. 13). The transit time in the reference Bragg cell

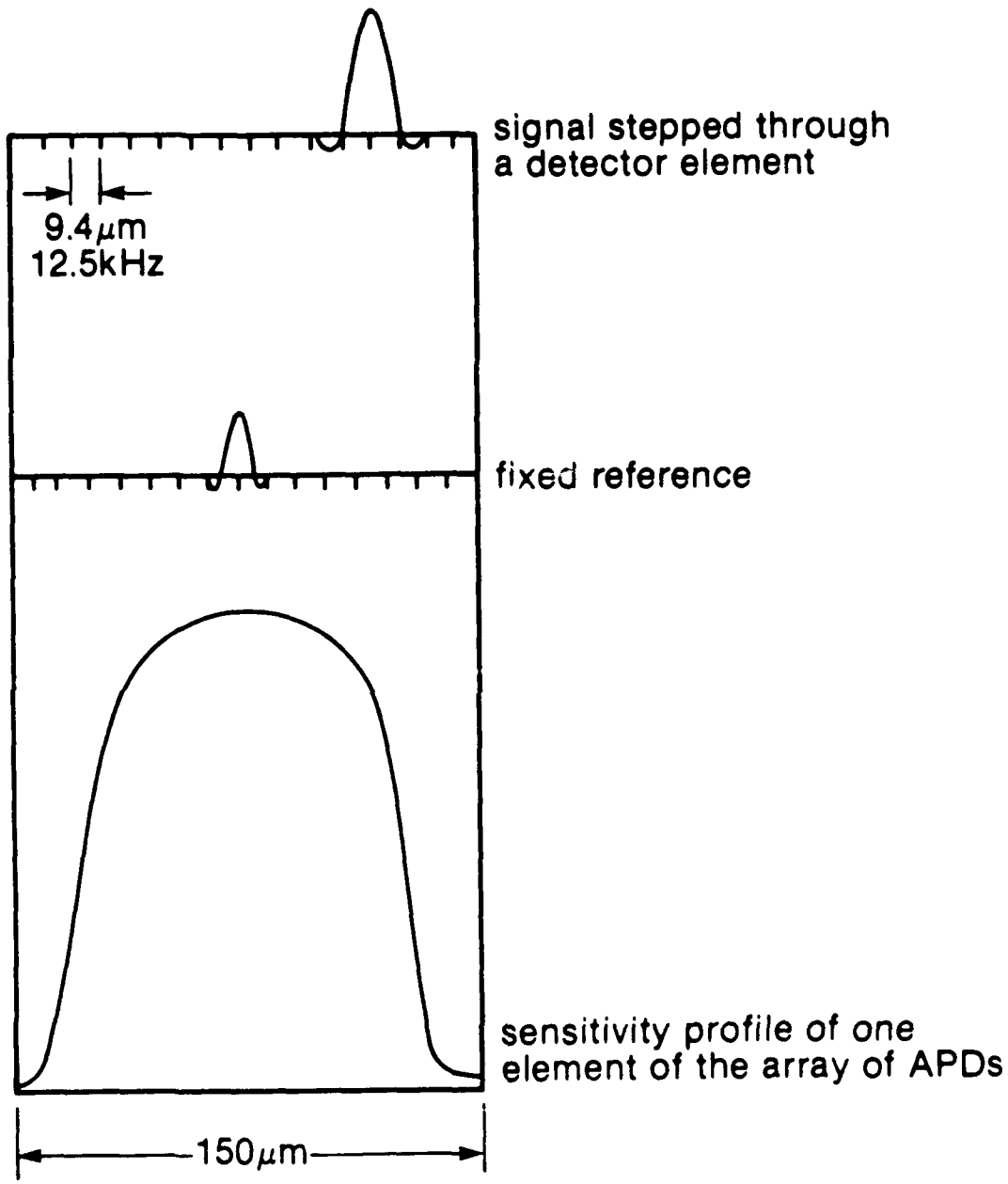

FIGURE 13: FOURIER PLANE OF AN ISA

(80 μs) is, as before, twice the transit time in the signal Bragg cell to ensure a resolution of 25 kHz. The focal length of the lens is 370 mm, so each element of the detector array (150 μm wide) sees a bandwidth of 200 kHz. The reference is a comb of frequencies separated by 200 kHz increments over the bandwidth of 51.2 MHz. Uniform frequency coverage is then achieved by stepping the signal in increments of 12.5 kHz. After 16 steps, the signal has been scanned over the 200 kHz bandwidth seen by each element of the detector array and the process can start again. Although only linear arrays of APDs with 32 element are available at this time, the utilization of two arrays of 128 elements each would produce a bandwidth of 51.2 MHz. A waiting time of 40 μs is necessary after each step while the signal fills the Bragg cell and a few more microseconds have to be added to account for the settling time of the local oscillator (LO).

There are advantages in leaving the reference fixed and stepping the signal. First, the transit time in the reference Bragg cell is twice the transit time in the signal Bragg cell, so stepping the signal allows twice the stepping rate than is possible by stepping the reference. Also, the sensitivity profile of the detecting elements of the APD array is not uniform [19]. Fig. 14a shows that the sensitivity is maximum at the centre of the elements and that they feature a sizable dead–space. Although the dead–space can be reduced by adding an array of specially designed lenses (see Fig. 14b), the technology is complex and will complicate development of a 128–element array. It is thus a distinct advantage to have a fixed reference that always uses the same section of each detecting element: the sensitivity profile on the edge of the elements is then irrelevant.

The bandwidth of the filter that follows each array element should be similar to the width of the diffraction spot (12.5 kHz) for each reference frequency to maintain good frequency resolution. Since a narrow detection bandwidth favors better dynamic range, it is one more advantage of using the SISA. However, the bandwidth of the filters has to be large enough to avoid the generation of frequency blind spots but small enough to enhance the frequency discrimination and noise rejection characteristics of the heterodyne detection process.

Generation of the reference signal is one of the most important and difficult parts of the operation of a SISA. In the particular case considered here, a comb of 256 tones, spaced by 200 kHz has to be produced. The frequency of each tone has to be stable and the amplitude of the tones across the bandwidth should be as uniform as possible while keeping the intermodulation products down. Let us consider the reference Bragg cell and define the detection threshold as the condition when the amplitude of the minimum detectable signal A_{SMIN} is equal to the amplitude of each reference frequency A_r (see Fig. 15). If A_{SMAX} is the maximum detectable signal, the following relation must exist between the parameters in order to obtain a 60 dB dynamic range:

$$\frac{A_{SMAX} \times A_r}{10^6} = A_{SMIN} \times A_r = A_r^2 \tag{5}$$

$$A_r = \frac{A_{SMAX}}{10^6} \tag{6}$$

Also, the amplitude of the intermodulation products between the reference tones has to be kept at least 60 dB below the level of the tones to ensure a dynamic range of 60 dB when heterodyne detection is utilized (see Fig. 15). This specification on the level of intermodulation products is very demanding, but the fact that the reference Bragg cell operates with a very low input level may make the implementation possible.

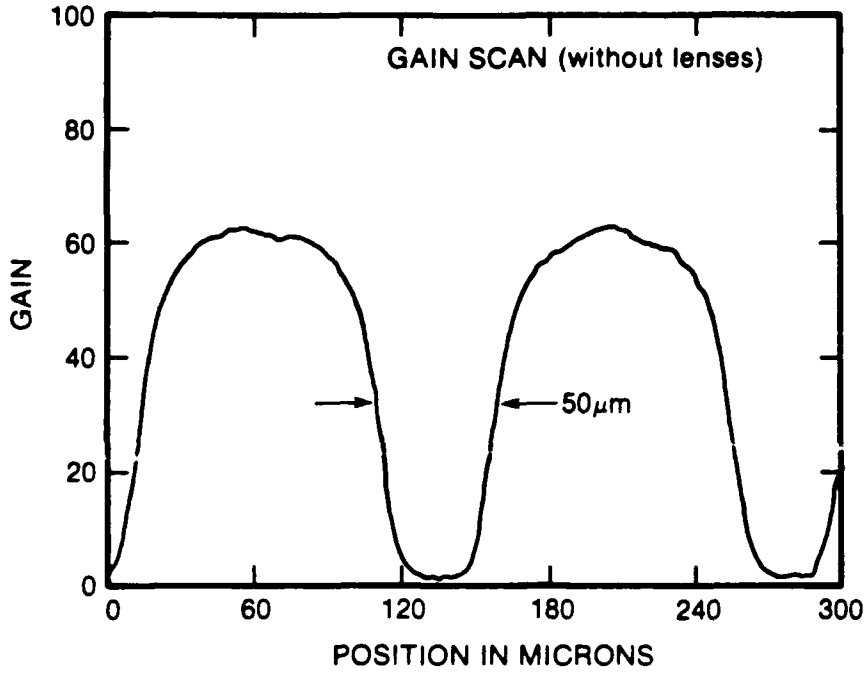

a)

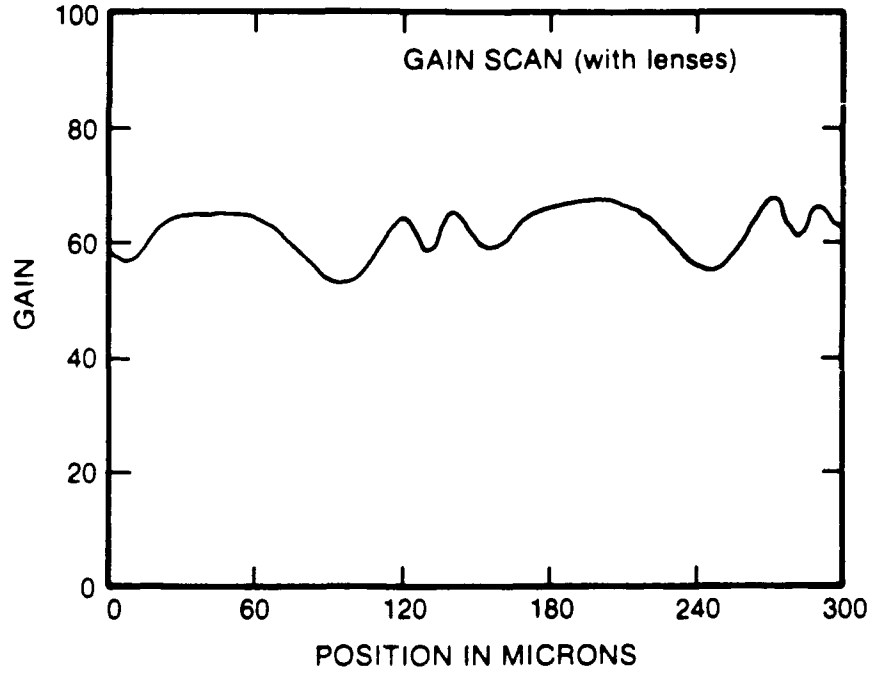

b)

FIGURE 14: SENSITIVITY PROFILE OF APDs
a) WITHOUT AN ARRAY OF LENS
b) WITH AN ARRAY OF LENS

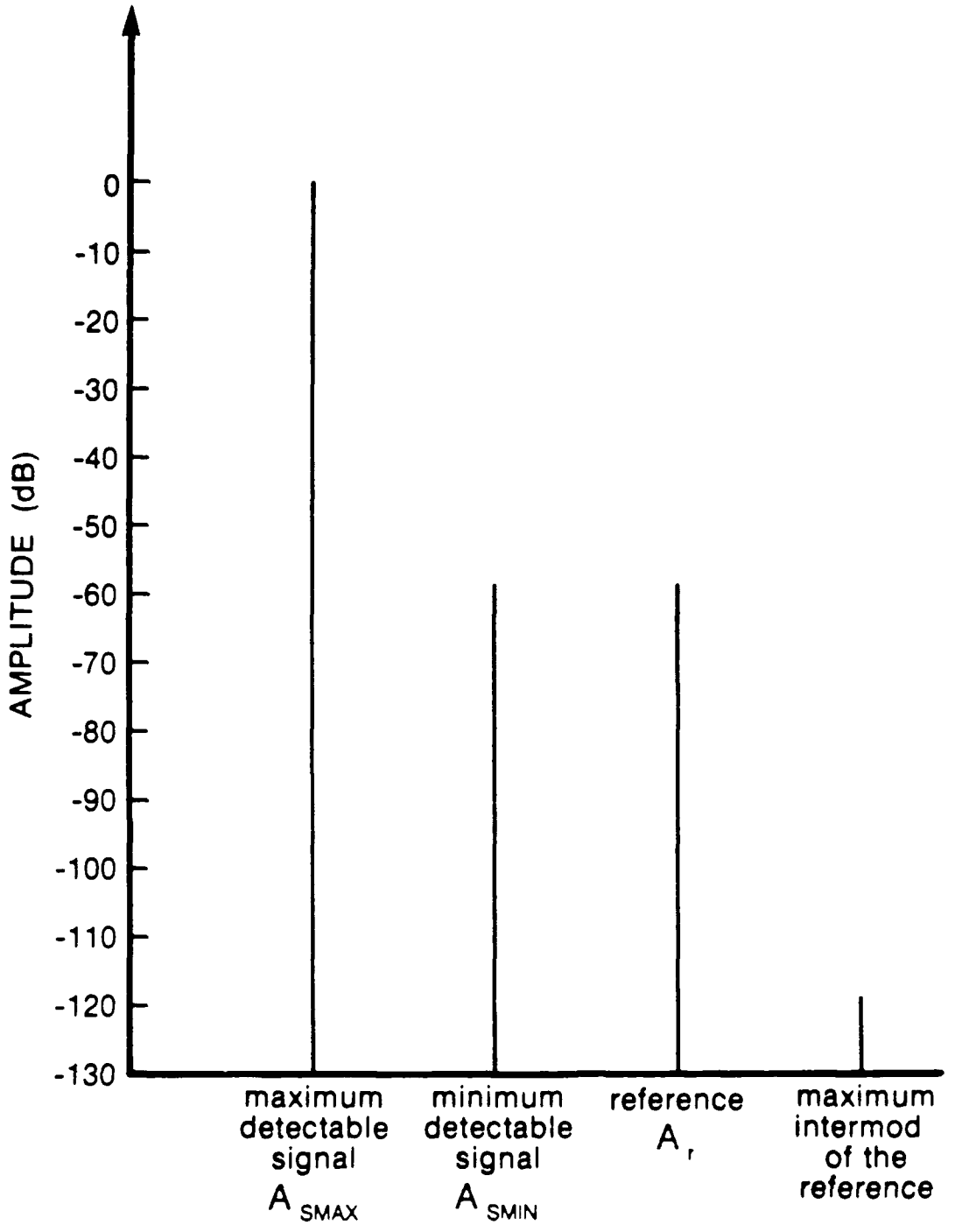

FIGURE 15: LEVELS OF THE REFERENCE AND SIGNAL INTERMODULATION PRODUCTS FOR A 60 dB DYNAMIC RANGE

The scanning process that permits the increased bandwidth consists of stepping through a 200 kHz bandwidth in sixteen steps of 12.5 kHz followed by either a reset to the starting frequency or the reverse process. The steps require sufficient accuracy to provide a regular, repeatable sweep that will not be blind to some frequency. There is always a minimum waiting time of 40 μs that is necessary to fill the signal Bragg cell after each step. The time required for the LO to settle after each frequency change influences the stepping rate, the length of the detection cycle and ultimately, the probability of detection for fast hoppers.

The operation of a high resolution large bandwidth SISA was described in the above section and some of the research and development that is foreseen in the implementation of the system was outlined. The next section contains an example calculation of the probability of detection for a specific set of parameters.

6.0 PROBABILITY OF DETECTION FOR A SCANNING INTERFEROMETRIC SPECTRUM ANALYSER

Before calculating of the probability of detection for a specific case, let us describe qualitatively the sequence of events associated with the scanning process and with the detection of a particular hop. It is useful to define a few parameters before starting:

T: duration of one hop,
t_h: starting time of a particular hop,
τ: transit time in the signal Bragg cell,
t_s: settling time of the LO generating the frequency steps
t_r: time between readings of the detector array
n: number of steps in a detection cycle,
δv: size of the frequency steps
$v_1, v_2, \ldots, v_N$: frequencies of the comb reference signal

At the beginning of a scan, the center frequency of the signal applied to the Bragg cell is set at v_0, at the center of the bandwidth of the signal Bragg cell. Then one has to wait for a time interval,

$$t_r = \tau + t_s \tag{7}$$

equal to the transit time in the Bragg cell plus the settling time of the LO before checking for the presence of a beat in each element of the detector array. So the signal levels at the frequencies $v_1, v_2, \ldots, v_N$ are measured. It will be assumed that it is possible to check instantly and in parallel all the detector elements involved in the system. Then the LO is stepped by one frequency increment δv. After another wait t_r, it is possible to check for the presence of signals at the frequencies $v_1+\delta v, v_2+\delta v, \ldots v_N+\delta v$. The LO moves one more step up and this time the signal levels at $n_1+2\delta v, n_2+2\delta v, \ldots, n_N+2\delta v$ are measured. This process is repeated n times until the bandwidth W_e associated with each detector element is scanned. W_e is equal to:

$$W_e = n\delta v \tag{8}$$

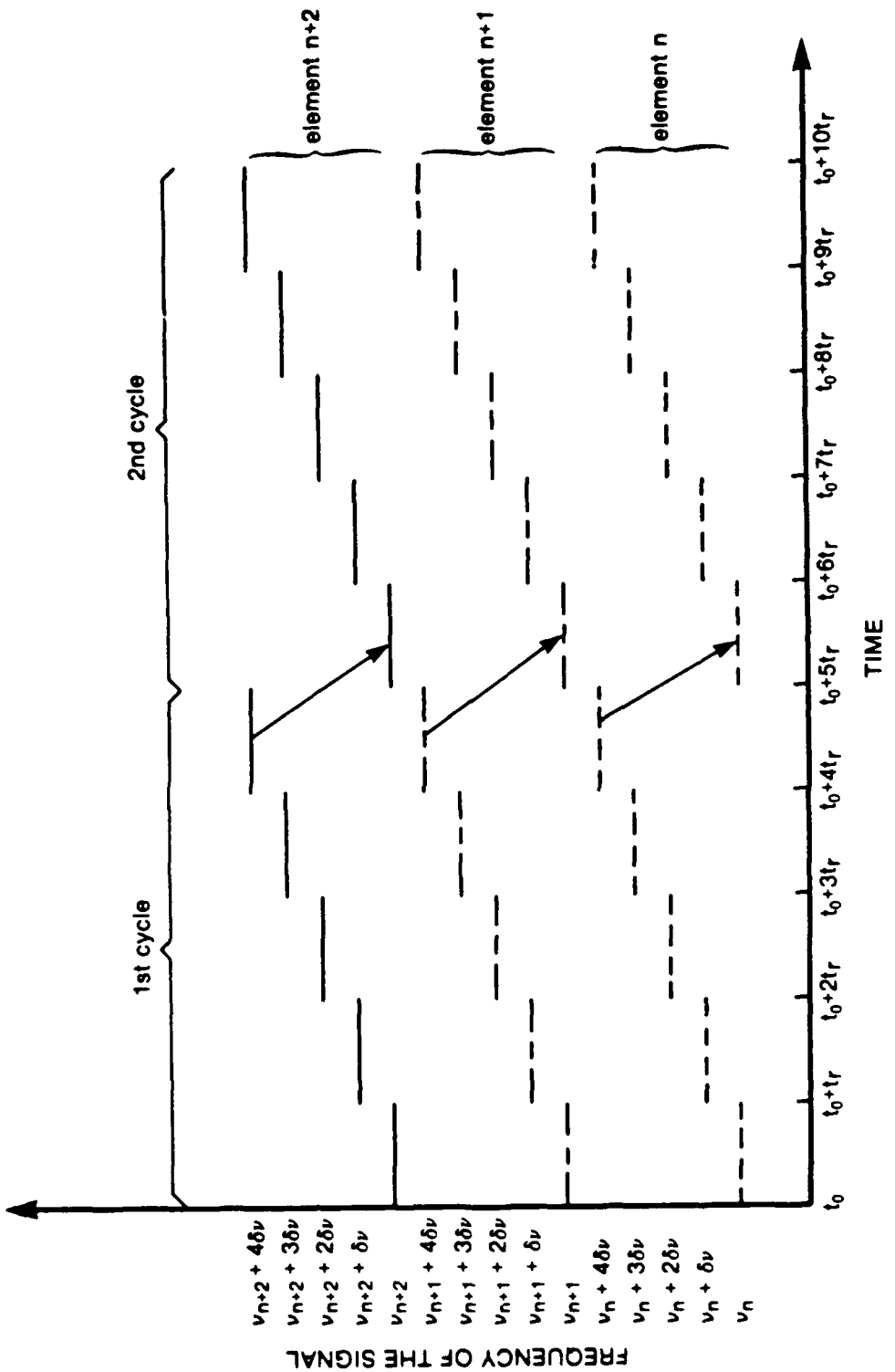

FIGURE 16: SCANNING PROCESS OF THE SISA

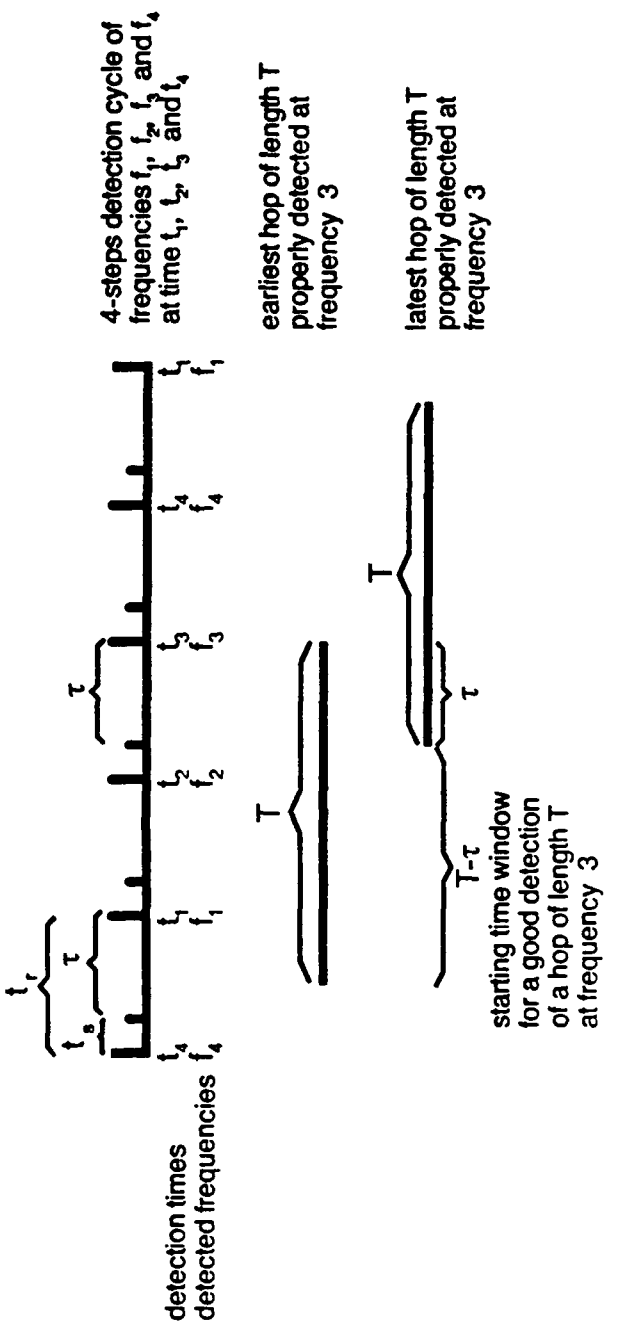

FIGURE 17: DETECTION OF A HOP BY A 4–STEPS DETECTION CYCLE

One test cycle is now finished and the process starts all over again when the LO is reset to the frequency v_o or when the scanning is done in the reverse direction. The scanning process is illustrated for three cycles, three elements and five steps in Fig. 16.

It will now be assumed that the hopper produces a CW signal of duration T starting at a certain time t_h. It takes a time τ for the signal to propagate through the Bragg cell and form a well shaped diffraction pattern. It also takes a time τ for the signal to leave the Bragg cell and during that time the diffraction pattern gradually diminishes in amplitude, broadens and finally disappears. So, although some detection is possible during the first and last segment τ of the signal, we will neglect it here: a detailed analysis of these transitory phenomena is beyond the scope of this study. We will consider the probability P of a good detection of a signal shorter than τ to be zero. At the other extreme, when the hop duration T is longer than the time $\tau+nt_r$ required to enter the Bragg and go through a detection cycle, we have

$$T > \tau + nt_r \tag{9}$$

and the probability of detection P is equal to one regardless of the relative phases of the hop sequence and the scanning process.

The transition between the almost zero probability of detection and the totally certain detection is interesting to study. Fig. 17 illustrates a 4–steps scanning process where the presence of signals at frequencies f_1, f_2, f_3 and f_4 is checked at times t_1, t_2, t_3 and t_4 respectively. The detection at time t_3 of a signal of length T at frequency f_3 is illustrated. In order to have a good detection, the signal must fill the Bragg cell aperture τ at the detection time t_3. The earliest time of arrival that will allow a good detection for a signal of length T detected at time t_3 is t_3–T. The latest time of arrival that will allow a good detection is t_3–τ. A time of arrival window of width W

$$W = T - \tau \tag{10}$$

is thus defined. If the starting time probability of a hop is uniform over one cycle, then the probability of detection of the hop is the ratio of the width W of the time–window to the length of the detection cycle. We then have

$$P = \frac{W}{n(t_s + \tau)} \tag{11}$$

and for different values of T, we have:

$$P = 1 \qquad \text{if } T > nt_r + \tau \tag{12}$$

$$P = \frac{T - \tau}{nt_r} \qquad \text{if } \tau < T < nt_r + \tau \tag{13}$$

$$P = 0 \qquad \text{if } T < \tau \tag{14}$$

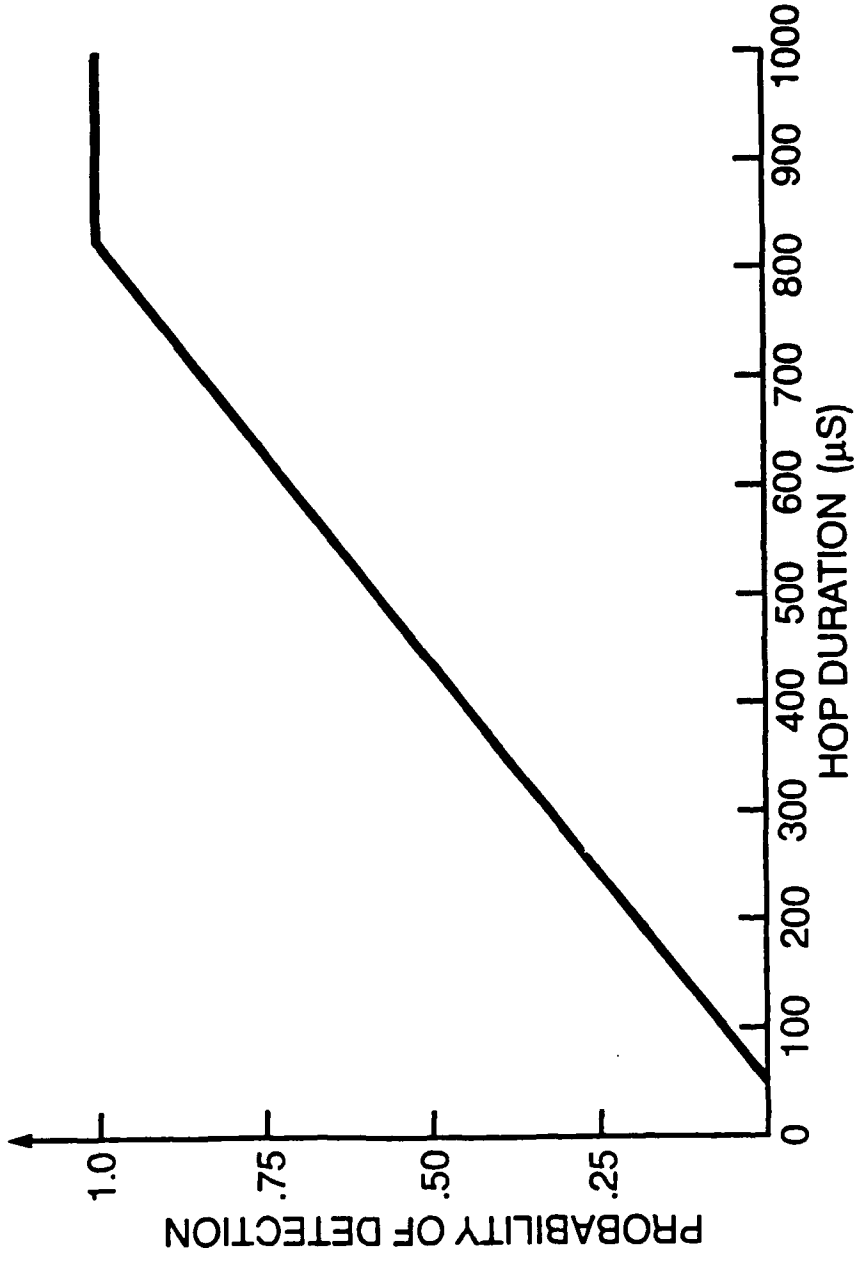

FIGURE 18: PROBABILITY OF HOP DETECTION AS A FUNCTION OF THE HOP DURATION T

Let us calculate a specific example with parameters drawn from Section 4. The transit time within the Bragg cell is 40 μs and the settling time of the LO is 10 μs, thus producing a time $t_r = 50\ \mu s$ between detector readings. The detection cycle is made of 16 steps of 12.5 kHz so each element of the detector array covers a bandwidth of 200 kHz in 800 μs. A total bandwidth of 51.2 MHz is covered if two 128–element detector arrays are used.

$\tau = 40\ \mu s$
$t_s = 10\ \mu s$
$t_r = 50\ \mu s$
$n = 16$
$\delta v = 12.5$ kHz
$\Delta v = 200$ kHz
$N = 256$ elements
$W = 51.2$ MHz

We have then from Eqs. 12, 13 and 14,

$$P = 1 \qquad \text{if } T > 840\ \mu s \tag{15}$$

$$P = \frac{T - 40}{50 \times 16} \qquad \text{if } 40\ \mu s < T < 840\ \mu s \tag{16}$$

$$P = 0 \qquad \text{if } T < 40\ \mu s \tag{17}$$

Fig. 18 shows the probability of detection P as a function of the length of the hop T. The transition between a probability of detection of one and zero is linear and a hopper operating at a rate less than 1190 hops/s (hop duration of more than 840 μs) will have a 100% probability of detection.

7.0 PROPOSAL FOR EXPERIMENTAL WORK ON SCANNING INTERFEROMETRIC SPECTRUM ANALYSERS

The successful development of a SISA would provide a much needed, high performances receiver for the detection of frequency hoppers. However, the scope and difficulty of the project are extensive and suggest a cautious approach. The starting point seems to be the testing of the TeO_2 Bragg cell's dynamic range. The 32–element array of APDs produced by RCA should be tested for dynamic range, sensitivity, detection threshold and cross–talk. It should then be possible to experimentally determine the drive level required of the reference signal generator and the feasibility of building such a generator. It should also be possible, after these initial tests, to define, from a computer model using the experimental data, the characteristics of the filters to be added after each element of the detector array. If the results of that preliminary work are sufficiently encouraging, the construction of a proof of concept system could be considered. It would be a SISA operating with a few elements, in order to be able to use commercial or in–house built signal generators. It would be wise at that stage to take advantage of the work done in RESM on read–out circuitry for the RCA arrays of APDs. If the performance of that system is satisfactory, then a decision will have to be made on the development of a fully operational laboratory prototype that should later be followed by the construction of a fieldable unit.

8.0 CONCLUSION

The concept of a high resolution, large dynamic range, large bandwidth acousto–optic spectrum analyser for the detection of frequency hoppers has been presented. The high resolution is produced by using Bragg cells with large transit times, while the large dynamic range results from a heterodyne detection process in an interferometric structure. The large bandwidth is achieved by a scanning process that put a limitation on the probability of detection of fast hoppers. A cautious, step–by–step approach was proposed to undertake exploratory work. If the tests on the Bragg cells demonstrate that they can produce the resolution and the dynamic range needed, a significant effort will be required to design a signal generator for the reference signal. Implementation of the frequency steps is an essential part of the scanning process and construction by RCA of 128–element APD arrays with appropriate read–out circuitry will be necessary.

9.0 REFERENCES

[1] A. Vander Lugt, "Interferometric Spectrum Analyser", Appl. Opt., Vol. 20, No. 16, 15 Aug. 1981, p. 2770–2779.

[2] A. Vander Lugt and A.M. Bardos, "Spatial and Temporal Spectra of Periodic Functions for Spectrum Analysis", Appl. Opt., Vol. 23, No. 23, 1 Dec 1984, p. 4269–4279.

[3] A. Vander Lugt, "Use of Decimated Photodetector Arrays in Spectrum Analysis", Appl. Opt., Vol. 27, No. 10, 15 May 1988, p. 2061–2070.

[4] J. Singh and R.M. De La Rue, "Observations of Intermodulation Effects in an Integrated Optical Spectrum Analyser", IEE Proc., Vol. 133, Pt. J, No. 1, Feb. 1986, p. 105–111.

[5] I.C. Chang, R. Lu and L.S. Lee, "High Dynamic Range Acousto–Optic Receivers", SPIE, Vol. 545, Optical Technology for Microwave Applications II, 1985, p. 95–101.

[6] J. Mellis, G.R. Adams and K.D. Ward, "High Dynamic Range Interferometric Bragg–Cell Spectrum Analyser", IEE Proc., Vol. 133, Pt.J, No. 1, Feb. 1986, p. 26–30.

[7] W.A. Wilby and P.V. Gatenby, "Theoretical Study of the Interferometric Bragg–Cell Spectrum Analyser", IEE Proc., Vol. 133, Pt. J., No. 1, Feb 1986, p. 47–59.

[8] T.S. Chen, S.K. Yao, S.C. Lin and D.J. Brunone, "Investigation of Large Dynamic Range Heterodyne Acousto–Optic Spectrum Analyser", SPIE, Vol. 477, Optical Technology for Microwave Applications I, 1984, p. 144–149.

[9] T.S. Chen and S.K. Yao, "Sensitivity, Noise and Optical Crosstalk in Heterodyne Acousto–Optical Signal Processors", SPIE, Vol. 545, Optical Technology for Microwave Applications II, 1985, p. 88–94.

[10] D.W. Graves and E. Lantz, "Decimated Photodetector Array Geometry in Spectrum Analysis: Experimental Results", SPIE vol. 936, Advances in Optical Information Processing III, 1988, p. 229–236.

[11] I.C. Change, "Acousto–Optic Channelized Receiver", Microwave Journal, March 1986, p. 141–157.

[12] M. Amano, G. Elston and J. Lucero, "Materials for Large Time Aperture Bragg Cell", SPIE, Vol. 567, Advances in Materials for Active Optics, 1985, p. 142–149.

[13] G. Elston, "Intermodulation Products in Acousto–Optic Signal Processing Systems", Ultrasonics Symposium, 1985, p. 391–397.

[14] S. Wolford, G. Petrie and D.L. Hecht, "Polarization Effects in Shear Wave Tellurium Dioxide Acousto–Optic Devices", SPIE, vol. 202, Active Optical Devices, 1979, p. 180–185.

[15] G. Elston, "Optically and Acoustically Rotated Slow Shear Bragg Cells in TeO_2", SPIE, vol. 936, Advances in Optical Information Processing III, 1988, p. 95–101.

[16] M.D. Koontz, "Miniature Interferometric Spectrum Analyser", SPIE, vol. 639, Optical Information Processing II, 1986, p. 126–130.

[17] J. B. Goodell, "Optical Design Considerations for Acousto–Optic Systems", SPIE, vol. 936, Advances in Optical Information Processing III, 1988, p. 22–28.

[18] A. Vander Lugt, "Decimated Arrays for Spectrum Analysis", SPIE vol. 936, Advances in Optical Information Processing III, 1988, p. 95–101.

[19] RCA Inc, "Development of a 32–Element Self Scanning Avalanche Photodiode Detector Array", Final Report, Contract No. 2SV85–00005, RCA Inc., New Products Division, Vaudreuil, Québec, Sept. 86.

[20] D.C. Sinclair and W.E. Bell, "Gas Laser Technology", Holt, Rinehart and Winston Inc., 1969, p. 39.

APPENDIX A

DOPPLER SHIFT OF THE DIFFRACTION PATTERNS FOR CW SIGNALS IN A BRAGG CELL

A good understanding of the temporal frequency distribution characteristics produced by CW signals and pulses is very important for the study of beat signal properties in an ISA. Four particular cases are analysed in detail following the procedure outlined in Ref. [7]. First, the case of CW signals filling the Bragg cell is considered, followed by the case of short pulses all within the cell. Finally, CW signals either entering or leaving the cell are studied.

If a signal s(t) is applied to a Bragg cell illuminated by a light distribution I(x), the complex light amplitude a(x,t) leaving the Bragg cell can be described [1] by a series

$$a(x,t) = I(x)\,[1 + jms(t-x/v) + H.O.T.] \qquad (A-1)$$

where m is the modulation index and v is the velocity of the acoustic wave within the cell. The undiffracted light, represented by the term I(x), does not carry any information. It is filtered out in the Fourier plane and ignored in the following calculations. The higher order terms (H.O.T.) are highly suppressed by the Bragg cell's mode of operation and can also be filtered out in the Fourier plane, so they are ignored too. From Eq. (A–1), the light amplitude distribution in the Fourier plane is then

$$A(p,t) = jm \int_{\infty}^{\infty} I(x)\, s(t-x/v)\, \exp(-j2\pi px)\, dx \qquad (A-2)$$

where p is the spatial frequency related to the physical distance ξ in the Fourier plane by

$$p = \xi/\lambda F \qquad (A-3)$$

where λ is the wavelength of the laser light and F is the focal length of the Fourier transform lens.

Let us assume that the signal s(t) applied to the Bragg cell is a sinusoidal waveform of frequency f_a and limited duration T described by

$$s(t) = \text{rect}\,\frac{(t-T/2)}{T}\,\exp(-j2\pi f_a t) \qquad (A-4)$$

and that the finite aperture of the Bragg cell τ, the Gaussian profile of the illumination pattern and the exponential attenuation in the Bragg cell a are described by an illumination function I(x) of the form

$$I(x) = \exp(-j2\pi f_o t)\,\text{rect}\frac{(x-L/2)}{L}\,\exp\frac{[-W(2x-L)^2]}{B}\,\exp[-a(f_a^2)x] \qquad (A-5)$$

where f_o is the temporal frequency of the illuminating light, L is the length of the Bragg cell, B is the width of the Gaussian beam profile at $1/e^2$ and W is the truncation ratio of the illumination. The exponential attenuation a depends on the square of the acoustic frequency f_a. A value of W = 0 describes a uniform illumination and a value of a = 0 describes a situation with no attenuation in the Bragg cell. Ignoring the jm term, the Fourier transform A(p,t) of the signal a(x,t) produced by the Bragg cell is then,

$$A(p,t) = \exp(-j2\pi f_o t) \int_{-\infty}^{\infty} \text{rect}\frac{(t-x/v-T/2)}{T} \exp[-j2\pi f_a(t-x/v)]$$

$$\text{rect}\frac{(x-L/2)}{L} \exp\frac{[-W(2x-L)^2]}{B} \exp[-a(f_a^2)x] \exp(-j2\pi px)\, dx \qquad \text{(A–6)}$$

Eq. (A–6) can be rewritten as

$$A(p,t) = \exp(-j2\pi f_o t) \exp(-j2\pi f_a t) \int_{L_1}^{L_2} \exp\frac{[-W(2x-L)^2]}{B} \exp[-a(f_a^2)x]$$

$$\exp[-j2\pi(p-p_a)x]\, dx \qquad \text{(A–7)}$$

where $p_a = f_a/v$ can be interpreted as the position of the centre of the diffraction pattern associated with an input signal at frequency f_a and $\Delta p = p-p_a$ is the distance from the centroid of the diffraction pattern. The values of L_1 and L_2 are determined by the rect functions of Eq. (A–6) and are the limiting values for the lower and upper limits of integration. This equation is easy to integrate for uniform illumination and no attenuation in the Bragg cell, that is when W and $a(f_a^2)$ are equal to zero. The effects of other values of W and a will be discussed at the end of this appendix. We then have

$$A(p,t) = \exp(-j2\pi f_o t) \exp(-j2\pi f_a t) \int_{L_2}^{L_1} \exp[-j2\pi(p-p_a)x]dx \qquad \text{(A–8)}$$

$$A(p,t) = \exp(-j2\pi f_o t) \exp(-j2\pi f_a t) \int_{-\infty}^{\infty} \text{rect}\frac{[x-(L_2+L_1)/2]}{L_2-L_1}$$

$$(\exp[-j2\pi(p-p_a)x]\ dx) \qquad \text{(A–9)}$$

$$A(p,t) = (L_2-L_1) \exp(-j2\pi f_o t) \exp(-j2\pi f_a t)$$

$$\exp[-j\pi(L_2+L_1)(p-p_a)]\ \text{sinc}[(L_2-L_1)(p-p_a)] \qquad \text{(A–10)}$$

Let us now consider the first case where two equal amplitude CW signals with frequencies f_a and f_b are filling the Bragg cell (see Fig. 2). We then have

$$L_1 = 0$$

$$L_2 = v\tau$$

so

$$L_2+L_1 = v\tau$$

$$L_2-L_1 = v\tau \qquad \text{(A–11)}$$

The light diffracted in the Fourier plane by the two CW signals is then

$$A_1(p,t) = v\tau \exp[-j2\pi(f_o+f_a)t] \exp[-j\pi(p-p_a)v\tau] \operatorname{sinc}[v\tau(p-p_a)]$$

$$+v\tau \exp[-j2\pi(f_o+f_b)t] \exp[-2\pi(p-p_b)v\tau] \operatorname{sinc}[v\tau(p-p_b)] \qquad \text{(A–12)}$$

The spectra of the two CW signals at frequencies f_a and f_b are two sinc functions of equal width and amplitude, centered at p_a and p_b respectively, with amplitudes it is proportional to τ (see Fig. 2). The amplitude and width of the sinc functions are independent of time and stay the same as long as the CW signals completely fill the Bragg cell. The sinc functions associated with the input CW signals at frequencies f_a and f_b, including the sidelobes, are respectively multiplied by the exponential phase factors $\exp(-j2\pi f_a t)$ and $\exp(-j2\pi f_b t)$. Since f_o is the frequency of the laser light illuminating the system, the two sinc functions oscillate at temporal frequencies of f_o+f_a and f_o+f_b.

Let us now consider the second case where two short pulses with durations t_a and t_b, lengths vt_a and vt_b, and frequencies f_a and f_b respectively, are entirely within the Bragg cell (see Fig. 3). Both the leading and trailing edges of the pulses are within the Bragg cell and the pulse centers are moving at the same velocity v as the acoustic wave. We then have

$$L_1 = (t-t_a)v \text{ or } (t-t_b)v$$

$$L_2 = vt$$

so

$$L_2+L_1 = (2t-t_a)v \text{ or } (2t-t_b)v$$

$$L_2-L_1 = vt_a \text{ or } vt_b \qquad \text{(A–13)}$$

The signal $A_2(p,t)$ in the Fourier plane can then be written as

$$A_2(p,t) = vt_a \exp(-j2\pi f_o t) \exp(-j2\pi f_a t) \exp[-j2\pi(p-p_a vt)] \exp[j\pi(p-p_a)vt_a]$$

$$\operatorname{sinc}[vt_a(p-p_a)]$$

$$+ vt_b \exp(-j2\pi f_o t) \exp(-j2\pi f_b t) \exp[-j2\pi(p-p_b)vt] \exp[j\pi(p-p_b)vt_b]$$

$$\operatorname{sinc}[vt_b(p-p_b)] \qquad \text{(A–14)}$$

$$A_2(p,t) = vt_a \exp[-j2\pi(f_o+f_a+v\Delta p_a)t] \exp(j\pi v\Delta p_a t_a)\operatorname{sinc}(vt_a\Delta p_a)$$

$$+ vt_b \exp[-j2\pi(f_o+f_b+v\Delta p_b)t]\exp(j\pi v\Delta p_b t_b)\operatorname{sinc}(vt_b\Delta p_b) \qquad \text{(A–15)}$$

where $\Delta p_a = p - p_a$ and $\Delta p_b = p - p_b$ are the distances in the frequency plane between the center of the diffraction patterns and the points where the temporal frequency is examined. The width and amplitude of the two sinc functions depend on t_a and t_b (see Fig. 3) and are constant in time as long as the pulses are entirely within the Bragg cell. The frequencies at p_a and p_b are f_o+f_a and f_o+f_b but the temporal frequency of the sidelobes at some spatial frequency $p=p_a+\Delta p_a$ is $f_o+f_a+\Delta f_a$ where $\Delta f_a = v\Delta p_a$. Similarly, for the signal b, the spatial frequency $p=p_b+\Delta p_b$ corresponds to a temporal frequency of $f_o+f_b+\Delta f_b$ where $\Delta f_b = v\Delta p_a$.

Let us now consider the third case where only the leading edge of two pulses are within the Bragg cell. The two pulses at frequencies f_a and f_b have entered the Bragg cell at times t_a and t_b respectively (see Fig. 4). The limits of integration are then

$$L_1 = 0$$

$$L_2 = v(t-t_a) \text{ or } v(t-t_b)$$

so

$$L_2+L_1 = v(t-t_a) \text{ or } v(t-t_b)$$

$$L_2-L_1 = v(t-t_a) \text{ or } v(t-t_b) \qquad \text{(A–16)}$$

The Fourier transform of the signal in the Bragg cell is then

$$A_3(p,t) = v(t-t_a)\exp(-j2\pi f_o t)\exp(-j2\pi f_a t)\exp[-j\pi(p-p_a)vt]\exp[j\pi(p-p_a)vt_a]$$
$$\text{sinc}[v(t-t_a)(p-p_a)]$$
$$+v(t-t_b)\exp(-j2\pi f_o t)\exp(-j2\pi f_b t)\exp[-j\pi(p-p_b)vt]\exp[j\pi(p-p_b)vt_b]$$
$$\text{sinc}[v(t-t_b)(p-p_b)] \qquad \text{(A–17)}$$

$$= v(t-t_a)\exp[-j2\pi(f_o+f_a+v\Delta p_a/2)t]\exp(j\pi v\Delta p t_a)\,\text{sinc}[v(t-t_a)\Delta p_a]$$
$$+v(t-t_b)\exp[-j2\pi(f_o+f_b+v\Delta p_b+v\Delta p_b/2)t)\exp(j\pi v\Delta p t_b)\,\text{sinc}(v(t-t_b)\Delta p_b \qquad \text{(A–18)}$$

From Eq. (A–1), the spectra of the two entering signals are centered at p_a and p_b respectively (see Fig. 4) and have different amplitudes and widths. The amplitudes and the widths are respectively linearly increasing and decreasing functions of time because the incoming signals are gradually filling the Bragg cell. The temporal frequencies at the centroids of each sinc are f_o+f_a and f_o+f_b like in the other cases, but the temporal frequencies of the sidelobes located at $p_a+\Delta p_a$ or $p_b+\Delta p_b$ are $f_o+f_a\Delta f_a/2$ and $f_o+f_b+\Delta f_b/2$ respectively where $f_a = v\Delta p_a$ and $f_b = v\Delta p_b$.

The situation for two pulses leaving the Bragg cell (see Fig. 5) is very similar. If the pulses started to leave the Bragg cell at t_a and t_b, the limits of integration are

$$L_1 = v(t-t_a) \text{ or } v(t-t_b)$$

$$L_2 = v\tau$$

so

$$L_2+L_1 = v(\tau+t-t_a) \text{ or } v(\tau+t-t_b)$$

$$L_2-L_1 = v(\tau-t+t_a) \text{ or } v(\tau-t+t_b) \qquad (A-19)$$

The Fourier transform is then

$$\begin{aligned} A_4(p,t) = {} & v(\tau-t+t_a)\exp(-j2\pi f_o t)\exp(-j2\pi f_a t)\exp[-j\pi t v(p-p_a)] \\ & \exp[-j\pi(\tau-t_a)v(p-p_a)]\,\mathrm{sinc}[v(\tau-t+t_a)(p-p_a)] \\ & +v(\tau-t+t_b)\exp(-j2\pi f_o t)\exp(-j2\pi f_b t)\exp[-j\pi t v(p-p_b)] \\ & \exp[-j\pi(\tau-t_b)v(p-p_b)]\,\mathrm{sinc}[v(\tau-t+t_b)(p-p_b)] \qquad (A-20) \end{aligned}$$

$$\begin{aligned} = {} & v(\tau-t+t_a)\exp[-j2\pi(f_o+f_a+v\Delta p_a/2)t]\exp[-j\pi(\tau-t_a)v\Delta p_a] \\ & \mathrm{sinc}[v(\tau-t+t_a)\Delta p_a] \\ & +v(\tau-t+t_b)\exp[-j2\pi(f_o+f_b+v\Delta p_b/2)t]\exp[-j\pi(\tau-t_b)v\Delta p_b] \\ & \mathrm{sinc}[v(\tau-t+t_b)\Delta p_b] \qquad (A-21) \end{aligned}$$

The spectra of the two leaving pulses are centered at p_a and p_b respectively (see Fig. 5) and have different amplitudes and widths. The amplitudes and widths are respectively linearly decreasing and increasing functions of time because the signals are leaving the Bragg cell. The temporal frequencies of the sidelobes located at $p_a+\Delta p_a$ or $p_b+\Delta p_b$ are $f_o+f_a+\Delta f_a/2$ and $f_o+f_b+\Delta f_b/2$ where $\Delta f_a = v\Delta p_a$ and $\Delta f_b = v\Delta p_b$.

The results can be summarized as follows. In all cases the temporal frequency of the light at the center of the diffraction pattern is shifted by the acoustic frequency of the signal in the Bragg cell. When the Bragg cell is filled with a CW signal, all the sidelobes of the diffraction pattern oscillate at the same temporal frequency as the center of the diffraction pattern. When both the leading and trailing edges of a pulse are within the Bragg cell, the temporal frequency of the sidelobes is no longer at the same frequency as the center of the diffraction pattern: at some spatial frequency $p_a+\Delta p$, the temporal frequency is $f_o+f_a+\Delta f$. Finally, when only the leading or the trailing edge of a pulse is within the Bragg cell, the temporal frequency of the sidelobes at a spatial frequency $p_a+\Delta p$ is $f_o+f_a+\Delta f/2$.

The exponential attenuation in the Bragg cell and the truncated Gaussian illumination could be accounted for at this stage by a convolution of the distributions A_1, A_2, A_3 and A_4 with the Fourier transform of the illumination profile and with the Fourier transform of the attenuation function. The nature of the temporal frequency distributions of the diffraction patterns is not changed by these operations.

APPENDIX B

EFFECTS OF THE He–Ne LASER'S MODE STRUCTURE ON THE OPERATION OF A HIGH RESULTION SISA

He–Ne lasers already available in the laboratory will be utilized in the early stages of work on the SISA. Although that type of laser operates in the fundamental transversal mode, the presence of many longitudinal modes is expected if special precautions are not taken. A Fourier transform exists for each of the wavelengths at which the laser operates, but the scale of the Fourier transform is slightly different for each wavelength. The elimination of all but one longitudinal mode can be achieved by many techniques. Unfortunately, in all cases, the useful output power of the laser is greatly reduced. The effects of the presence of many longitudinal modes on the SISA's performance can be calculated.

The width of the gain curve (see Fig. 19) for a He–Ne laser operating at 633 nm is 1.7 GHz [20]. The frequency difference δf between adjacent longitudinal modes is given by

$$\delta f = \frac{c}{2L} \qquad \text{(B–1)}$$

where c is the velocity of light and L is the length of the laser cavity. For a 1 m long laser, δf is equal to 150 MHz. The modes can exist only if located within a frequency band where there is enough gain to reach the lasing threshold of the laser. A maximum of 11 modes are possible for a 1 m long laser cavity. The maximum change in wavelength associated with a 1.7 GHz bandwidth can be found from the basic relation between the velocity, frequency and wavelength of light:

$$c = \lambda v \qquad \text{(B–2)}$$

The derivative of Eq. (B–2) gives

$$\Delta\lambda = \lambda^2 \frac{\Delta v}{c} \qquad \text{(B–3)}$$

It can then be easily calculated that a 1.7 GHz change in frequency produces a wavelength of 2.3×10^{-12} m in a 1 m long He–Ne laser. The position of a particular frequency in the Fourier plane depends on

$$\frac{\Delta F}{2\Lambda} \qquad \text{(B–4)}$$

where F is the focal length of the lens performing the Fourier transform and Λ is the wavelength of the acoustic wave in the Bragg cell. If F is equal to 370 mm, in the worst case, for Λ equal to 6.8 μm (100 MHz input to the Bragg cell), there is a position change in the Fourier plane of less than .07 μm. The resolution of the system is 12.5 kHz which corresponds to a distance of 9.4 μm in the Fourier plane. A position change of .07 μm is thus negligible and a multi–longitudinal mode He–Ne laser can be used to illuminate the SISA.

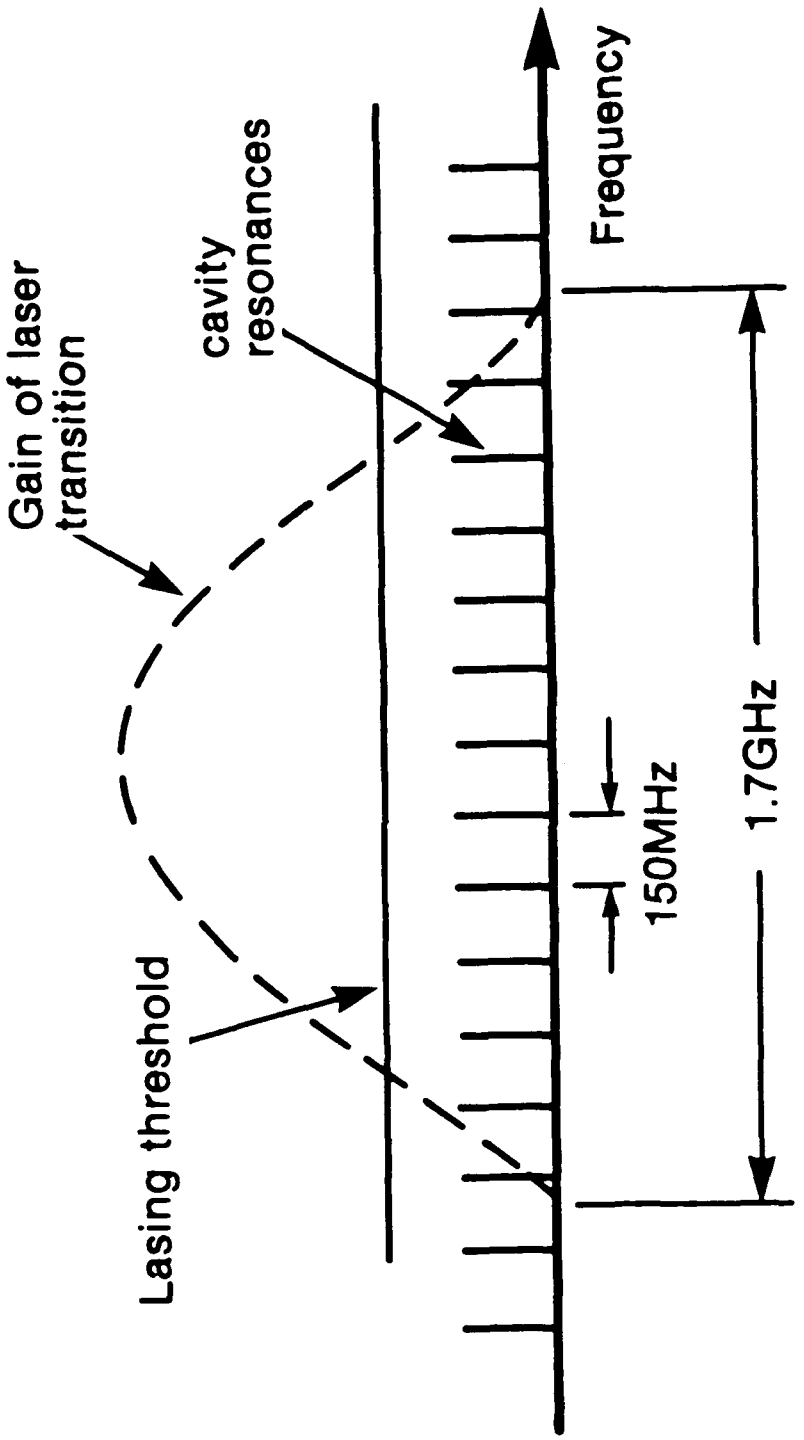

FIGURE 19: LONGITUDINAL MODE STRUCTURE OF A He–Ne LASER WITH A 1 m LONG CAVITY

DOCUMENT CONTROL DATA

(Security classification of title, body of abstract and indexing annotation must be entered when the overall document is classified)

1. ORIGINATOR (the name and address of the organization preparing the document. Organizations for whom the document was prepared, e.g. Establishment sponsoring a contractor's report, or tasking agency, are entered in section 8.)

NATIONAL DEFENCE
DEFENCE RESEARCH ESTABLISHMENT OTTAWA
SHIRLEY BAY, OTTAWA, ONTARIO K1A 0Z4 CANADA

2. SECURITY CLASSIFICATION (overall security classification of the document. including special warning terms if applicable)

UNCLASSIFIED

3. TITLE (the complete document title as indicated on the title page. Its classification should be indicated by the appropriate abbreviation (S,C,R or U) in parentheses after the title.)

DEFINITION OF THE CONCEPT OF AN INTERFEROMETRIC SPECTRUM ANALYSER FOR THE DETECTION OF FREQUENCY HOPPING RADIOS (U)

4. AUTHORS (Last name, first name, middle initial)

BROUSSEAU, NICOLE

5. DATE OF PUBLICATION (month and year of publication of document)

JANUARY 1991

6a. NO. OF PAGES (total containing information. Include Annexes, Appendices, etc.)

53

6b. NO. OF REFS (total cited in document)

20

7. DESCRIPTIVE NOTES (the category of the document, e.g. technical report, technical note or memorandum. If appropriate, enter the type of report, e.g. interim, progress, summary, annual or final. Give the inclusive dates when a specific reporting period is covered.)

DREO TECHNICAL NOTE

8. SPONSORING ACTIVITY (the name of the department project office or laboratory sponsoring the research and development. Include the address.)

NATIONAL DEFENCE
DEFENCE RESEARCH ESTABLISHMENT OTTAWA
OTTAWA, ONTARIO K1A 0Z4 CANADA

9a. PROJECT OR GRANT NO. (if appropriate, the applicable research and development project or grant number under which the document was written. Please specify whether project or grant)

041LK11

9b. CONTRACT NO. (if appropriate, the applicable number under which the document was written)

10a. ORIGINATOR'S DOCUMENT NUMBER (the official document number by which the document is identified by the originating activity. This number must be unique to this document.)

DREO TECHNICAL NOTE 90-20

10b. OTHER DOCUMENT NOS (Any other numbers which may be assigned this document either by the originator or by the sponsor)

11. DOCUMENT AVAILABILITY (any limitations on further dissemination of the document, other than those imposed by security classification)

(XX) Unlimited distribution
( ) Distribution limited to defence departments and defence contractors; further distribution only as approved
( ) Distribution limited to defence departments and Canadian defence contractors; further distribution only as approved
( ) Distribution limited to government departments and agencies; further distribution only as approved
( ) Distribution limited to defence departments; further distribution only as approved
( ) Other (please specify):

12. DOCUMENT ANNOUNCEMENT (any limitation to the bibliographic announcement of this document. This will normally correspond to the Document Availability (11). However, where further distribution (beyond the audience specified in 11) is possible, a wider announcement audience may be selected.)

UNCLASSIFIED

SECURITY CLASSIFICATION OF FORM

13. ABSTRACT (a brief and factual summary of the document. It may also appear elsewhere in the body of the document itself. It is highly desirable that the abstract of classified documents be unclassified. Each paragraph of the abstract shall begin with an indication of the security classification of the information in the paragraph (unless the document itself is unclassified) represented as (S), (C), (R), or (U). It is not necessary to include here abstracts in both offical languages unless the text is bilingual).

(U) The concept of a high resolution, large bandwidth and high dynamic range acousto-optic spectrum analyser for the detection of frequency hoppers is described. The high resolution is achieved by the selection of large time aperture Bragg cells while the high dynamic range is obtained by the utilization of heterodyne detection in an interferometric structure. The large bandwidth is produced by a scanning process. An example of the probability of detection for a specific selection of parameters is given.

14. KEYWORDS, DESCRIPTORS or IDENTIFIERS (technically meaningful terms or short phrases that characterize a document and could be helpful in cataloguing the document. They should be selected so that no security classification is required. Identifiers, such as equipment model designation, trade name, military project code name, geographic location may also be included. If possible keywords should be selected from a published thesaurus, e.g. Thesaurus of Engineering and Scientific Terms (TEST) and that thesaurus-identified. If it is not possible to select indexing terms which are Unclassified, the classification of each should be indicated as with the title.)

Spectrum analyser
Acousto-Optic
TeO_2 Bragg Cell

UNCLASSIFIED

SECURITY CLASSIFICATION OF FORM